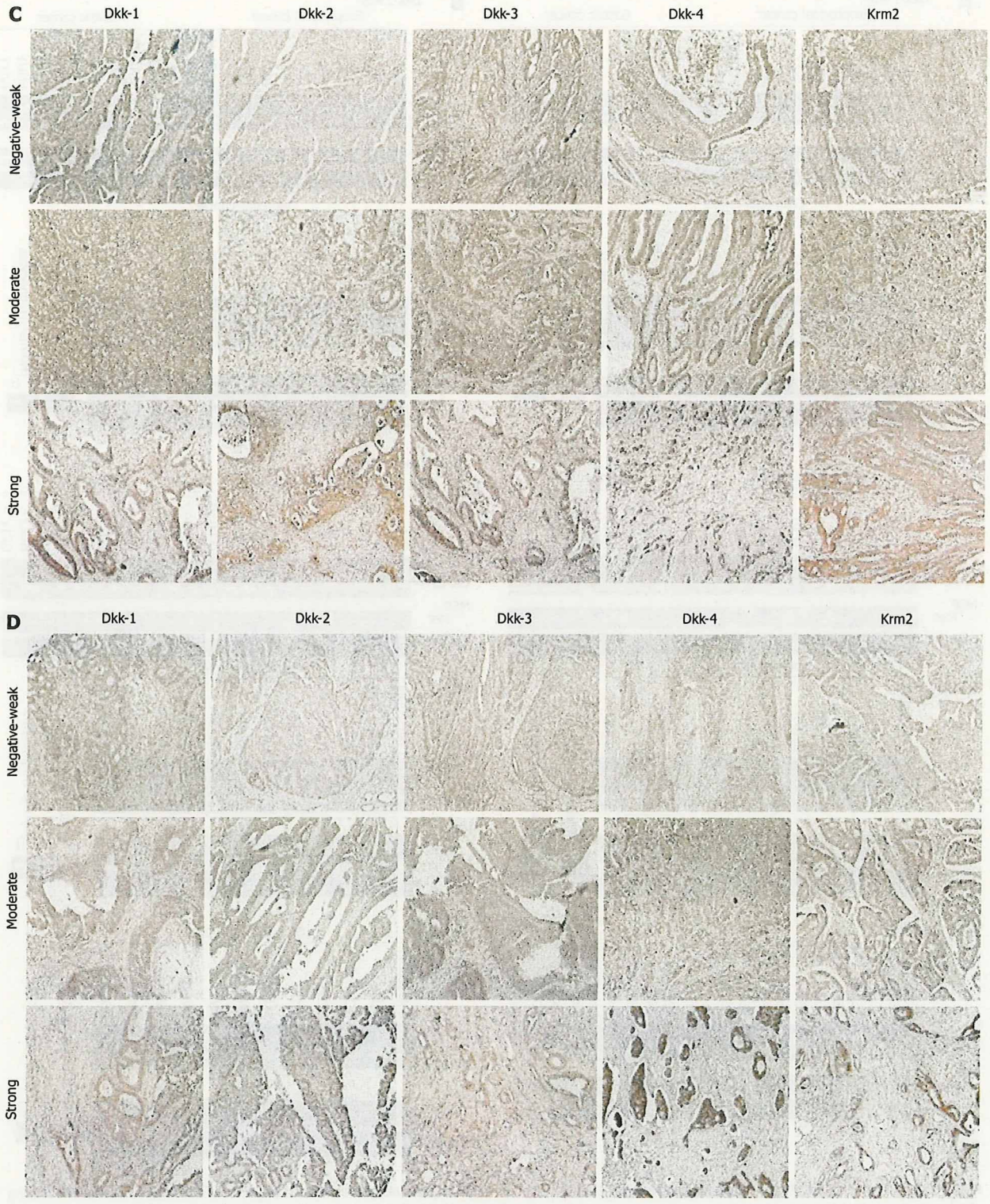

Figure 3 Immunohistochemical expression of Dkks in gastrointestinal normal and cancer tissues. **A:** Normal tissues; **B:** Esophageal cancer tissues; **C:** Gastric cancer tissues; **D:** Colorectal cancer tissues (× 200).

6/60 (10.0%) of colorectal cancer tissues, respectively. On the other hand, strong staining of Dkk-1, Dkk-2, Dkk-3, Dkk-4, and Krm2 was found in 28/59 (47.5%), 9/59 (15.3%), 10/59 (16.9%), 28/59 (47.5%) and 11/59 (18.6%) of esophageal cancer tissues, in 15/60 (25.0%), 14/60 (23.3%), 22/59 (37.3%), 33/59 (55.9%) and 7/60 (11.7%) of gastric cancer tissues, and in 10/60 (16.7%), 12/60 (20.0%), 6/60 (10.0%), 35/60 (58.3%) and 28/60 (46.7%) of colorectal cancer tissues, respectively (Figure 3B-D and data not shown). Expression levels of Dkks and Krm2

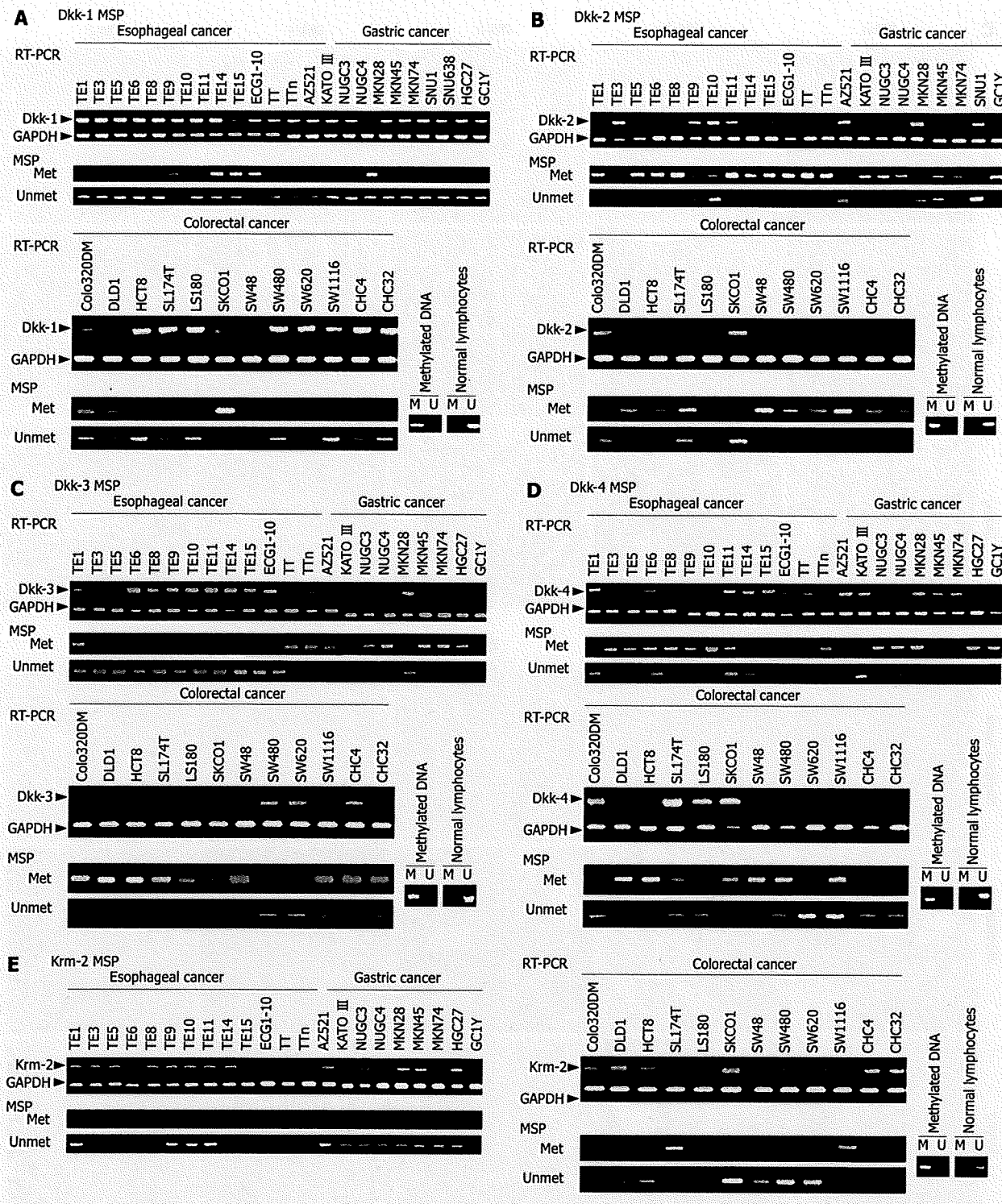

Figure 5 Correlation of methylation in the promoter region with silencing of the Dkk genes in gastrointestinal cancer cell lines. RT-PCR and MSP were carried out using cDNA and genomic DNA from the indicated cancer cell lines, respectively. *In vitro* methylated DNA (CpG Genome Universal Methylated DNA from Chemicon International, Temecula, CA) was used as a positive control for methylated alleles, while DNA from normal lymphocytes was used as negative controls.

were not correlated with any of the clinicopathological characteristics. However, in colorectal cancers with beta-catenin over-expression, Dkk-1 expression levels were significantly lower in those with lymph node metastasis than in those without lymph node metastasis ($P = 0.003$).

CpG island hypermethylation of the Dkk subfamily genes in gastrointestinal cancer

Using Blast and CpG island searcher, we found that Dkk-1, Dkk-2, Dkk-3, and Krm2 genes contain CpG islands at their 5'ends and that Dkk-4 has a few CpGs in the

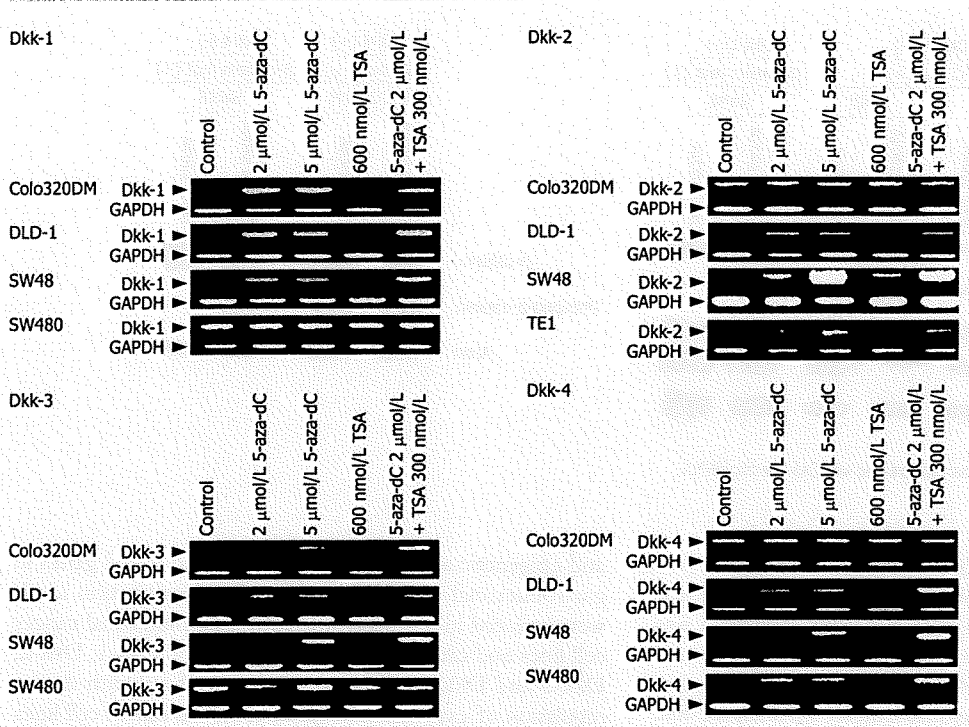

Figure 6 Reactivation of Dkks expression by 5-aza-dC treatment in gastrointestinal cancer cell lines. Cells were treated indicated.

promoter region (Figure 4). Therefore, we analyzed the methylation status of the CpG islands of these genes in cancer cell lines and tissue samples using MSP. Methylation status was significantly associated with silencing of Dkks mRNA expression in cancer cell lines (Figure 5 and data not shown). Methylation status was associated with silencing of Krm2 mRNA expression in only some cancer cell lines, such as LS174T and SW1116 cells (Figure 5E). In cancer tissues, Dkk-1, Dkk-2, Dkk-3, and Dkk-4 were hypermethylated in 4/11 (36.4%), 1/11(9.1%), 1/11 (9.1%) and 3/11 (27.3%) of esophageal cancer tissues, in 2/8 (25.0%), 2/8 (25.0%), 2/8 (25.0%) and 3/8 (37.5%) of gastric cancer tissues, and in 7/20 (35.0%), 13/20 (65.0%), 7/20 (35.0%) and 4/20 (20.0%) of colorectal cancer tissues, respectively (data not shown).

To confirm the role of epigenetic change in silencing of the Dkk genes, cell lines that lacked the Dkk genes expression were treated with 5-aza-dC and/or TSA. Treatment with 5-aza-dC resulted in restoration of Dkk-1 in colo320DM, DLD-1, and SW48 cells, restoration of Dkk-2 expression in DLD-1, SW48, and TE1 cells, restoration of Dkk-3 expression in colo320DM and DLD-1 cells, and restoration of Dkk-4 expression in DLD-1, SW48, and SW480 cells (Figure 6). However, treatment with TSA had no effect.

Correlations between expression levels of Dkks and those of canonical and non-canonical Wnt pathway signal genes in gastrointestinal cancer

There were some binding motifs of beta-catenin (5'-YCTTTGWW-3') in the promoter regions of Dkk-1 and Dkk-4. Dkk-2, Dkk-3 and Krm2 did not have TCF-binding motifs in their promoter regions. There were significant correlations between levels of Dkk-1, Dkk-3, Dkk-4 and Krm2 and those of beta-catenin expression in colorectal cancer tissues in tissue microarray data obtained by immunohistochemistry. Dkk-1 ($r = 0.500$, $P < 0.0001$), Dkk-3 ($r = 0.326$, $P = 0.0130$), Dkk-4 ($r = 0.480$, $P = 0.0003$) and Krm2 ($r = 0.454$, $P = 0.0005$) expression levels showed significant correlations with beta-catenin over-expression. However, no correlation was found between expression levels of these molecules and beta-catenin over-expression in gastric or esophageal cancer tissues (data not shown). We then analyzed expression levels of beta-catenin and phosphorylated beta-catenin in Dkk1 or Dkk4-specific siRNA-treated colon cancer cells with APC mutation (SW480, WiDr, and colo320DM cells) and SW48 cells with beta-catenin mutation using Western blot analysis. SW480 and WiDr cells treated with Dkk1-specific siRNA showed higher levels of beta-catenin expression and lower levels of phosphorylated beta-catenin compared with those of the control siRNA-treated cells (Figure 7). On the other hand, Dkk-1-negative SW48 cells treated with Dkk1-specific siRNA showed no difference compared with the control cells. Colo320DM cells treated with Dkk4-specific siRNA showed higher levels of beta-catenin expression and lower levels of phosphorylated beta-catenin compared with those of the control siRNA-treated cells (Figure 7). On the other hand, Dkk4-negative SW48 cells treated with Dkk4-specific siRNA showed no difference compared with the control cells.

Next, we examined expression of Rac and phosphorylated Rac/CDC42, which Wnt4/5A/11 activates through Dvl, and CaMKII and phosphorylated CaMKII to investigate the effects on Wnt-PCP and Wnt-Ca^{2+} signal transduction. Expression of Rac, phospho-Rac, CaMKII, and phospho-CaMKII was not correlated with any of the clinicopathological features. Rac activation ratio ((phospho-Rac) level-(Rac) level/(Rac)level) was negatively correlated with Dkk-1 in colorectal cancer ($r = -0.366$, $P = 0.0053$)

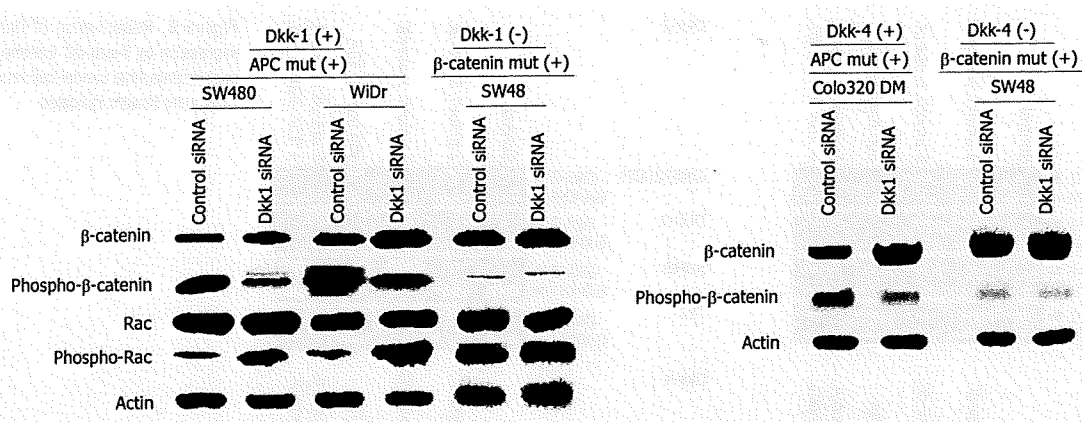

Figure 7 Western blot analysis in cancer cells treated with Dkk-specific siRNA.

and with Dkk-2 (r = -0.290, P = 0.0299) and Dkk-3 (r = -0.3880, P = 0.0037) in esophageal cancer, but not in gastric cancer. On the other hand, CaMKII activation ratio was positively correlated with Dkk-2 (r = 0.285, P = 0.0314) and Krm2 (r = 0.3640, P = 0.0075) in esophageal cancer, but not in colorectal cancer or gastric cancer. We analyzed Rac expression level and the phosphorylation status of Rac in cells treated with Dkk1-specific siRNA using Western blot analysis. SW480 and WiDr cells treated with Dkk1-specific siRNA showed similar expression levels of Rac and higher levels of phosphorylated Rac compared with those of cells treated with the control siRNA (Figure 7). On the other hand, Dkk-1-negative SW48 cells treated with Dkk1-specific siRNA showed no difference compared with the control cells.

Enhancement of cancer cell growth and invasiveness by Dkk-1, Dkk-2, Dkk-3, or Dkk-4 siRNA treatment

WST-8 assays and *in vitro* invasion assays after treatment with specific siRNA for the Dkk genes were performed to assess the role of the expression of Dkks in cancer cell growth and invasiveness. Transfection with siRNA resulted in over 80% inhibition of mRNA and protein expression (data not shown). Transfection with Dkk1-specific siRNA enhanced the growth of SW480 and WiDr cells compared with control siRNA-transfected counterparts (Figure 8A; $P < 0.01$). Transfection with Dkk2-, Dkk3- and Dkk4-specific siRNA enhanced the growth of TE9, SW480 and colo320DM cells compared with control siRNA-transfected counterparts, respectively (Figure 8A; $P < 0.05$, $P < 0.001$ and $P < 0.001$). Transfection with Dkk-1, Dkk-3, or Dkk-4-specific siRNA enhanced the invasiveness of TE-1 cells compared with control siRNA-transfected counterparts (Figure 8B and C $P < 0.01$). Transfection with Dkk-1 or Dkk-3-specific siRNA enhanced the invasiveness of TE-8 cells compared with control siRNA-transfected counterparts (Figure 8B and C, $P < 0.01$). Transfection with Dkk-1-specific siRNA enhanced the invasiveness of SW480 cells compared with control siRNA-transfected counterparts (Figure 8B and C, $P < 0.01$).

DISCUSSION

In the present study, we investigated the expression profiles and epigenetic alterations of the Dkks and Krm2 genes in gastrointestinal cancer. Dkks and Krm2 expression levels were reduced in a certain subset of gastrointestinal cancer cell lines and cancer tissues. Methylation of Dkk-1, Dkk-2, Dkk-3 and Dkk-4 was significantly correlated with down-regulation of expression in gastrointestinal cancer cell lines and cancer tissues. Moreover, Dkk-1, Dkk-2, Dkk-3 and Dkk-4 mRNA expression was restored by treatment with the DNA-demethylating agent. These results suggest that promoter hypermethylation is an important mechanism of silencing of Dkk family in gastrointestinal cancer. Although there were only a few CpGs in the Dkk-4 promoter region, these CpG sites in cancer tissues were more methylated than in normal tissues. Similarly, the expression of rat placental lactogen-1 (rPL-I) has been reported to be controlled by DNA methylation although the gene has only 17 CpG sites in the 5'-flanking region[25].

Over-expression of Dkk-1, Dkk-2, Dkk-3 and Dkk-4 was also found in a subset of gastrointestinal cancer tissues. This is not a surprising result, because of the following reasons. There are binding motifs of beta-catenin in the promoter regions of Dkk-1 and Dkk-4. Multiple beta-catenin/TCF4 sites in the Dkk-1 gene promoter have been reported to contribute to Dkk-1 activation, thus initiating a negative feedback loop[5]. In fact, Dkk-1 mRNA levels have been increased in a subset of colorectal cancer tissues compared to normal tissues[5]. In our study, Dkk-1, Dkk-3, Dkk-4 and Krm2 expression was correlated with beta-catenin over-expression in colorectal cancer tissues. Moreover, knockdown of Dkk-1 or Dkk-4 up-regulated levels of beta-catenin expression and down-regulated levels of phosphorylated beta-catenin. Therefore, Dkks and Krm2 could be directly and/or indirectly induced by Wnt signals, at least in part, as components of negative feedback loops; but, this mechanism may be lost or abolished in a certain subset of colorectal cancers by promoter hypermethylation. On the other hand, no correlation was found between expression levels of Dkks and Krm2 and beta-catenin over-expression in gastric or esophageal cancer tissues. Further analysis is required to clarify the mechanism of over-expression of Dkks and Krm2 in a subset of gastric and esophageal cancers.

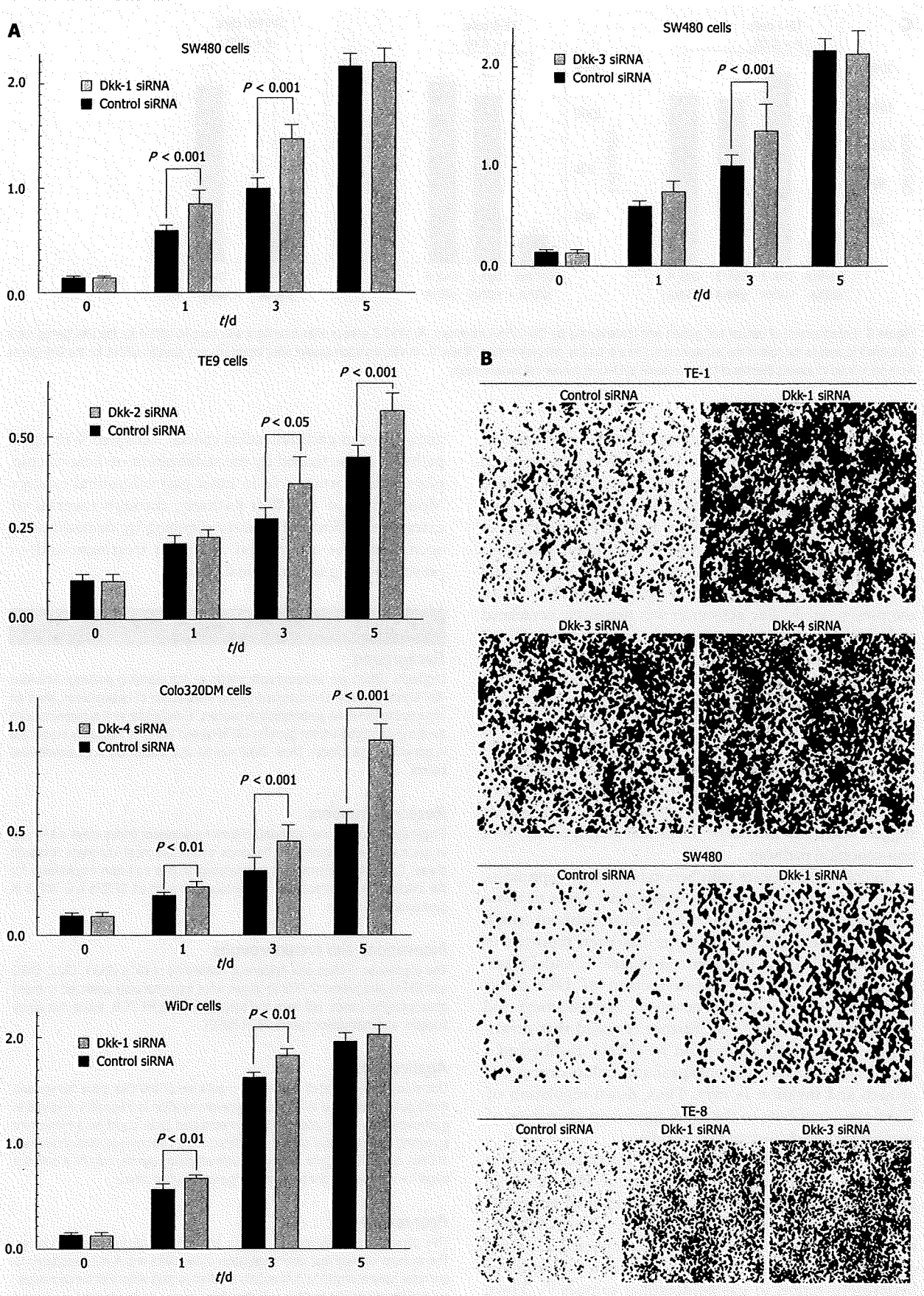
A
SW480 cells
Dkk-1 siRNA
Control siRNA
P < 0.001
P < 0.001
2.0
1.0
0.0
0
1
3
5
t/d
SW480 cells
Dkk-3 siRNA
Control siRNA
P < 0.001
2.0
1.0
0.0
0
1
3
5
t/d
TE9 cells
Dkk-2 siRNA
Control siRNA
P < 0.001
P < 0.05
0.50
0.25
0.00
0
1
3
5
t/d
Colo320DM cells
Dkk-4 siRNA
Control siRNA
P < 0.001
P < 0.001
P < 0.01
1.0
0.5
0.0
0
1
3
5
t/d
WiDr cells
Dkk-1 siRNA
Control siRNA
P < 0.01
P < 0.01
2.0
1.0
0.0
0
1
3
5
t/d
B
TE-1
Control siRNA
Dkk-1 siRNA
Dkk-3 siRNA
Dkk-4 siRNA
SW480
Control siRNA
Dkk-1 siRNA
TE-8
Control siRNA
Dkk-1 siRNA
Dkk-3 siRNA

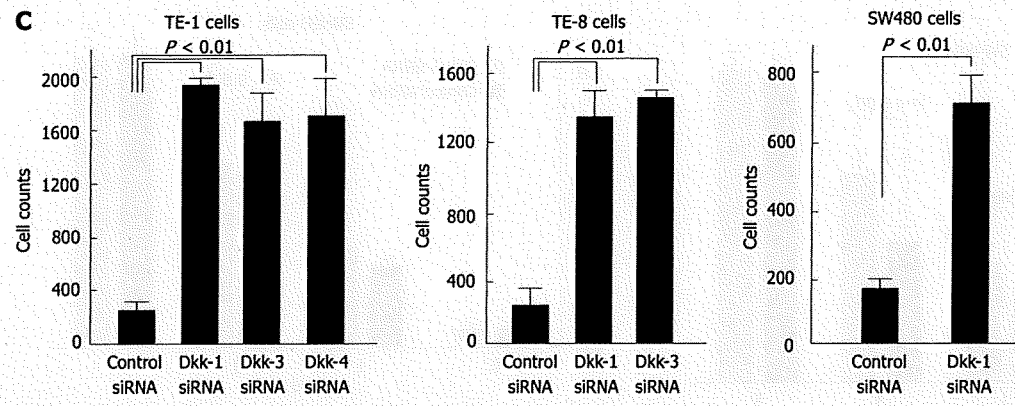

Figure 8 Enhancement of cancer cell growth and invasiveness by Dkk siRNA treatment. **A**: WST-8 assays after treatment with specific siRNA for the Dkk genes were performed to assess the role of the expression of Dkks in cancer cell proliferation; **B** and **C**: *In vitro* invasion assays after treatment with specific siRNA for the Dkk genes were performed to assess the role of the expression of Dkks in cancer cell invasiveness.

Next, we examined correlations of altered expression of Dkks and Krm2 with expression of the Wnt non-canonical pathway genes. It has been reported that the Wnt canonical pathway activation stabilizes beta-catenin and that the non-canonical pathway activates Rho, Rac, JNK, and PKC or activates CaMK II [26]. The TAK1-NLK MAPK cascade is activated by the non-canonical Wnt-5A/Ca^{2+} pathway and antagonizes canonical Wnt/beta-catenin signaling[27,28]. In the present study, Rac activation was negatively correlated with Dkk-1 expression in colorectal cancer and with Dkk-2 and Dkk-3 in esophageal cancer. These results suggest that Dkk-1 down-regulation in colorectal cancer and Dkk-2 or Dkk-3 down-regulation in esophageal cancer play a role in Rac activation. Moreover, knockdown of Dkk-1 using Dkk-1-specific siRNA induced Rac phosphorylation. On the other hand, CaMK II activation showed a weak positive correlation with Dkk-2 and Krm2 in esophageal cancer. Although further investigation is required, these results suggest additional effects of Dkks and Krm2 on the Wnt non-canonical pathway.

In colorectal cancers with beta-catenin over-expression, Dkk-1 expression levels were significantly lower in those with lymph node metastasis than in those without lymph node metastasis. Dkk-1 promoter has been reported to be hypermethylated in advanced Dukes' C and Dukes' D colorectal cancers[7]. Transfection of Dkk-3 has been reported to reduce invasion of osteosarcoma and malignant melanoma[9]. We further revealed that down-regulation of Dkks expression by siRNA resulted in a significant increase in esophageal and colon cancer cell growth and invasion *in vitro*. Thus, down-regulation of Dkks may contribute to the more aggressive phenotype of esophageal and colorectal cancer cells.

Our results indicate that promoter hypermethylation is an important mechanism of silencing of Dkk family in gastrointestinal cancer. Suzuki *et al*[29,30] reported epigenetic inactivation of secreted frizzled-related proteins (sFRPs) in colorectal and gastric cancer. We reported silencing of the Wnt inhibitory factor-1 gene due to promoter hypermethylation in gastrointestinal tumors[18]. Thus, CpG island promoter hypermethylation is a common mechanism of the inactivation of extracellular Wnt antagonists in gastrointestinal cancer. Activated Wnt signal pathway, characterized by the stabilization of beta-catenin, plays an important role in most gastrointestinal cancers. Modulation of the Wnt pathway, through reversal of extracellular Wnt antagonists silencing by demethylating agents, may be a potential target for treatment and/or prevention of gastrointestinal cancer.

COMMENTS

Background

Dickkopfs (Dkks) are secreted antagonists of Wnt signaling pathway. Activated Wnt signal pathway, characterized by the stabilization of beta-catenin, plays an important role in most gastrointestinal cancers. Extracellular Wnt antagonists such as secreted frizzled-related proteins (SFRPs) and WIF-1 is frequently inactivated in gastrointestinal cancer. Thus, Dkks may be also inactivated in gastrointestinal cancer.

Research frontiers

Epigenetic transcriptional silencing of tumor suppressor genes plays a key role in gastrointestinal cancer and becomes one of the most important research areas. CpG island promoter hypermethylation is a common mechanism for the inactivation of extracellular Wnt antagonists such as SFRPs and WIF-1 in gastrointestinal cancer.

Innovations and breakthroughs

The expression profiles and epigenetic alterations of Dkks (Dkk1, Dkk2, Dkk3 and Dkk4) and Kremen2 (Krm2) genes were systematically analyzed in many gastrointestinal cancer cell lines and tissues by using RT-PCR, tissue microarray analysis, and methylation specific PCR (MSP).

Applications

Our study demonstrated that down-regulation of the Dkk gene family and Krm2 gene associated to promoter hypermethylation is frequently involved in gastrointestinal tumorigenesis. Hypermethylated Dkks could be a marker for screening gastrointestinal cancer. Modulation of the Wnt pathway, through reversal of Dkks and/or Krm2 gene silencing by demethylating agents, may be a potential target for treatment and/or prevention of gastrointestinal cancer.

Peer review

This paper studied alterations of Dkks and Krm2 in gastrointestinal cancer. The authors showed that down-regulation of the Dkks and Krm2 associated to promoter hypermethylation is frequently involved in gastrointestinal tumorigenesis. Hypermethylated Dkks could be a marker for screening gastrointestinal cancer and reactivation of Dkks and/or Krm2 gene could be a promising strategy for treatment and/or prevention of gastrointestinal cancer.

REFERENCES

1 **Kawano Y**, Kypta R. Secreted antagonists of the Wnt signalling pathway. *J Cell Sci* 2003; **116**: 2627-2634
2 **Katoh M**, Katoh M. WNT signaling pathway and stem cell signaling network. *Clin Cancer Res* 2007; **13**: 4042-4045
3 **Glinka A**, Wu W, Delius H, Monaghan AP, Blumenstock C, Niehrs C. Dickkopf-1 is a member of a new family of secreted proteins and functions in head induction. *Nature* 1998; **391**: 357-362
4 **Krupnik VE**, Sharp JD, Jiang C, Robison K, Chickering TW, Amaravadi L, Brown DE, Guyot D, Mays G, Leiby K, Chang B, Duong T, Goodearl AD, Gearing DP, Sokol SY, McCarthy SA. Functional and structural diversity of the human Dickkopf gene family. *Gene* 1999; **238**: 301-313
5 **Gonzalez-Sancho JM**, Aguilera O, Garcia JM, Pendas-Franco N, Pena C, Cal S, Garcia de Herreros A, Bonilla F, Munoz A. The Wnt antagonist DICKKOPF-1 gene is a downstream target of beta-catenin/TCF and is downregulated in human colon cancer. *Oncogene* 2005; **24**: 1098-1103
6 **Wang J**, Shou J, Chen X. Dickkopf-1, an inhibitor of the Wnt signaling pathway, is induced by p53. *Oncogene* 2000; **19**: 1843-1848
7 **Aguilera O**, Fraga MF, Ballestar E, Paz MF, Herranz M, Espada J, Garcia JM, Munoz A, Esteller M, Gonzalez-Sancho JM. Epigenetic inactivation of the Wnt antagonist DICKKOPF-1 (DKK-1) gene in human colorectal cancer. *Oncogene* 2006; **25**: 4116-4121
8 **Lee AY**, He B, You L, Xu Z, Mazieres J, Reguart N, Mikami I, Batra S, Jablons DM. Dickkopf-1 antagonizes Wnt signaling independent of beta-catenin in human mesothelioma. *Biochem Biophys Res Commun* 2004; **323**: 1246-1250
9 **Kuphal S**, Lodermeyer S, Bataille F, Schuierer M, Hoang BH, Bosserhoff AK. Expression of Dickkopf genes is strongly reduced in malignant melanoma. *Oncogene* 2006; **25**: 5027-5036
10 **Mao B**, Wu W, Davidson G, Marhold J, Li M, Mechler BM, Delius H, Hoppe D, Stannek P, Walter C, Glinka A, Niehrs C. Kremen proteins are Dickkopf receptors that regulate Wnt/beta-catenin signalling. *Nature* 2002; **417**: 664-667
11 **Mao B**, Niehrs C. Kremen2 modulates Dickkopf2 activity during Wnt/LRP6 signaling. *Gene* 2003; **302**: 179-183
12 **Nozaki I**, Tsuji T, Iijima O, Ohmura Y, Andou A, Miyazaki M, Shimizu N, Namba M. Reduced expression of REIC/Dkk-3 gene in non-small cell lung cancer. *Int J Oncol* 2001; **19**: 117-121
13 **Tsuji T**, Nozaki I, Miyazaki M, Sakaguchi M, Pu H, Hamazaki Y, Iijima O, Namba M. Antiproliferative activity of REIC/Dkk-3 and its significant down-regulation in non-small-cell lung carcinomas. *Biochem Biophys Res Commun* 2001; **289**: 257-263
14 **Kobayashi K**, Ouchida M, Tsuji T, Hanafusa H, Miyazaki M, Namba M, Shimizu N, Shimizu K. Reduced expression of the REIC/Dkk-3 gene by promoter-hypermethylation in human tumor cells. *Gene* 2002; **282**: 151-158
15 **Roman-Gomez J**, Jimenez-Velasco A, Agirre X, Castillejo JA, Navarro G, Barrios M, Andreu EJ, Prosper F, Heiniger A, Torres A. Transcriptional silencing of the Dickkopfs-3 (Dkk-3) gene by CpG hypermethylation in acute lymphoblastic leukaemia. *Br J Cancer* 2004; **91**: 707-713
16 **Hsieh SY**, Hsieh PS, Chiu CT, Chen WY. Dickkopf-3/REIC functions as a suppressor gene of tumor growth. *Oncogene* 2004; **23**: 9183-9189
17 **Katoh Y**, Katoh M. Comparative genomics on DKK2 and DKK4 orthologs. *Int J Mol Med* 2005; **16**: 477-481
18 **Taniguchi H**, Yamamoto H, Hirata T, Miyamoto N, Oki M, Nosho K, Adachi Y, Endo T, Imai K, Shinomura Y. Frequent epigenetic inactivation of Wnt inhibitory factor-1 in human gastrointestinal cancers. *Oncogene* 2005; **24**: 7946-7952
19 **Hirata T**, Yamamoto H, Taniguchi H, Horiuchi S, Oki M, Adachi Y, Imai K, Shinomura Y. Characterization of the immune escape phenotype of human gastric cancers with and without high-frequency microsatellite instability. *J Pathol* 2007; **211**: 516-523
20 **Herman JG**, Graff JR, Myohanen S, Nelkin BD, Baylin SB. Methylation-specific PCR: a novel PCR assay for methylation status of CpG islands. *Proc Natl Acad Sci USA* 1996; **93**: 9821-9826
21 **Cameron EE**, Bachman KE, Myohanen S, Herman JG, Baylin SB. Synergy of demethylation and histone deacetylase inhibition in the re-expression of genes silenced in cancer. *Nat Genet* 1999; **21**: 103-107
22 **Taniguchi H**, Yamamoto H, Akutsu N, Nosho K, Adachi Y, Imai K, Shinomura Y. Transcriptional silencing of hedgehog-interacting protein by CpG hypermethylation and chromatic structure in human gastrointestinal cancer. *J Pathol* 2007; **213**: 131-139
23 **Miyamoto N**, Yamamoto H, Taniguchi H, Miyamoto C, Oki M, Adachi Y, Imai K, Shinomura Y. Differential expression of angiogenesis-related genes in human gastric cancers with and those without high-frequency microsatellite instability. *Cancer Lett* 2007; **254**: 42-53
24 **Yamamoto H**, Vinitketkumnuen A, Adachi Y, Taniguchi H, Hirata T, Miyamoto N, Nosho K, Imsumran A, Fujita M, Hosokawa M, Hinoda Y, Imai K. Association of matrilysin-2 (MMP-26) expression with tumor progression and activation of MMP-9 in esophageal squamous cell carcinoma. *Carcinogenesis* 2004; **25**: 2353-2360
25 **Cho JH**, Kimura H, Minami T, Ohgane J, Hattori N, Tanaka S, Shiota K. DNA methylation regulates placental lactogen I gene expression. *Endocrinology* 2001; **142**: 3389-3396
26 **Katoh M**. WNT/PCP signaling pathway and human cancer (review). *Oncol Rep* 2005; **14**: 1583-1588
27 **Ishitani T**, Ninomiya-Tsuji J, Nagai S, Nishita M, Meneghini M, Barker N, Waterman M, Bowerman B, Clevers H, Shibuya H, Matsumoto K. The TAK1-NLK-MAPK-related pathway antagonizes signalling between beta-catenin and transcription factor TCF. *Nature* 1999; **399**: 798-802
28 **Ishitani T**, Kishida S, Hyodo-Miura J, Ueno N, Yasuda J, Waterman M, Shibuya H, Moon RT, Ninomiya-Tsuji J, Matsumoto K. The TAK1-NLK mitogen-activated protein kinase cascade functions in the Wnt-5a/Ca(2+) pathway to antagonize Wnt/beta-catenin signaling. *Mol Cell Biol* 2003; **23**: 131-139
29 **Suzuki H**, Watkins DN, Jair KW, Schuebel KE, Markowitz SD, Chen WD, Pretlow TP, Yang B, Akiyama Y, Van Engeland M, Toyota M, Tokino T, Hinoda Y, Imai K, Herman JG, Baylin SB. Epigenetic inactivation of SFRP genes allows constitutive WNT signaling in colorectal cancer. *Nat Genet* 2004; **36**: 417-422
30 **Nojima M**, Suzuki H, Toyota M, Watanabe Y, Maruyama R, Sasaki S, Sasaki Y, Mita H, Nishikawa N, Yamaguchi K, Hirata K, Itoh F, Tokino T, Mori M, Imai K, Shinomura Y. Frequent epigenetic inactivation of SFRP genes and constitutive activation of Wnt signaling in gastric cancer. *Oncogene* 2007; **26**: 4699-4713

S- Editor Zhong XY **L- Editor** Negro F **E- Editor** Yin DH

Carcinogenesis vol.29 no.3 pp.666–672, 2008
doi:10.1093/carcin/bgn001
Advance Access publication January 19, 2008

Further upregulation of β-catenin/Tcf transcription is involved in the development of macroscopic tumors in the colon of *Apc*$^{Min/+}$ mice

Takeru Oyama, Yasuhiro Yamada*, Kazuya Hata, Hiroyuki Tomita, Akihiro Hirata[1], HongQiang Sheng, Akira Hara, Hitomi Aoki[2], Takahiro Kunisada[2], Satoshi Yamashita[3] and Hideki Mori

Department of Tumor Pathology, Gifu University Graduate School of Medicine, 1-1 Yanagido, Gifu 501-1194, Japan, [1]Division of Animal Experiment, Life Science Research Center, Gifu University, Yanagido 1-1, Gifu, 501-1193, Japan, [2]Department of Tissue and Organ Development, Regeneration and Advanced Medical Science, Gifu University Graduate School of Medicine, Gifu 501-1194, Japan and [3]Carcinogenesis Division, National Cancer Center Research Institute, 5-1-1 Tsukiji, Chuo-ku, Tokyo, Japan

*To whom correspondence should be addressed.
Email: y-yamada@gifu-u.ac.jp

$Apc^{Min/+}$ mouse, a mouse model for human familial adenomatosis polyposis, contains a truncating mutation in the *Apc* gene and spontaneously develops intestinal tumors. Our previous study revealed two distinct stages of tumorigenesis in the colon of $Apc^{Min/+}$ mouse: microadenomas and macroscopic tumors. Microadenomas already have lost their remaining allele of the *Apc* and all microadenomas show accumulation of β-catenin, indicating that activation of the canonical Wnt pathway is an initiating event in the tumorigenesis. This study shows that expression of nuclear β-catenin in macroscopic tumors is further upregulated in comparison with that in microadenomas. Furthermore, transcriptional activity of β-catenin/T-cell factor (Tcf) signaling, assessed using β-catenin/Tcf reporter transgenic mice, is higher in the macroscopic tumors than that in microadenomas. In addition, the expression level of Dickkopf-1, which is known to be a negative modifier of the canonical Wnt pathway, was reduced only in colon tumors. These results suggest that activation of β-catenin/Tcf transcription plays a role not only in the initiation stage but also in the promotion stage of colon carcinogenesis in $Apc^{Min/+}$ mice.

Introduction

Colorectal carcinogenesis is a multistep process (1). In humans, *APC*, *KRAS* oncogene and *p53* genes are thought to play important roles at different stages of colorectal carcinogenesis (2,3). Of these, mutations in the *APC* gene found in the earliest stages of the adenoma–carcinoma sequence are recognized to play a gate-keeping role in tumor formation and progression (4). Moreover, germ line mutations in the *APC* gene are known to be responsible for familial adenomatous polyposis, a dominantly inherited autosomal condition characterized by the formation of multiple colonic adenomatous polyps with a high likelihood to develop colon carcinomas (5,6).

A mutant mouse lineage predisposed to Min is regarded as one of the models for colorectal tumorigenesis (7). Originally, this lineage was established from an ethylnitrosourea-treated C57BL/6J mouse. The dominant mutation is known to be located in *Apc*, the mouse homologue of the human *APC* gene, resulting in truncation of the gene product at amino acid 850 (8). $Apc^{Min/+}$ mice develop multiple intestinal neoplasia in the intestinal tracts. Therefore, *APC* is now regarded as a tumor suppressor gene, and inactivation of both alleles is considered to be necessary for tumor formation (9). In mice heterozygous for a mutant allele of *Apc*, the loss of *Apc* function occurs almost exclusively by LOH (10,11).

Abbreviations: Dkk1, Dickkopf-1; PBS, phosphate-buffered saline; PCR, polymerase chain reaction; RT–PCR, reverse transcription—polymerase chain reaction; Tcf, T-cell factor.

$Apc^{Min/+}$ mice have been reported to develop intestinal tumors primarily in their small intestine and only a few tumors arise in the colon (12). Our previous study revealed the presence of a number of intramucosal microadenomas (~100 microadenomas) in the colon of $Apc^{Min/+}$ mice (12). In that study, microadenomas in the colon of the $Apc^{Min/+}$ mice consisted of a few dysplastic crypts (12). Based on the multistep carcinogenesis theory in the colon (2–4), such findings suggested that there are, at least, two distinct stages for colon tumorigenesis in $Apc^{Min/+}$ mice. Importantly, such microadenomas in the colon were found to have lost the remaining allele of *Apc*, thus indicating that a loss of the *Apc* function has already occurred in such crypts (12–14). In agreement with the presence of *Apc* LOH, the accumulation of β-catenin is observed in all microadenomas in the colon of the $Apc^{Min/+}$ mice (12). These findings suggest that activation of the Wnt signaling pathway by *Apc* LOH is the initiating event in the carcinogenesis but is not sufficient for the development of macroscopic tumors.

It is not clear at this time which event is required for the development of macroscopic tumors in the colon of $Apc^{Min/+}$ mice. Although it has been reported that K-*ras*, *p53* and B-*raf* genes are sometimes mutated in colorectal cancers and such alterations are expected to cause progression of colon carcinogenesis (2), no genetic alterations of these genes are detected in colon tumors of the $Apc^{Min/+}$ mice model (unpublished data).

The purpose of this study was to identify alterations that are responsible for the development of macroscopic tumors in the colon of $Apc^{Min/+}$ mice. It is possible that the increased expression of the canonical Wnt pathway, accompanied by an increased nuclear β-catenin level and a decreased Dickkopf-1 (Dkk1) expression, is associated with the development of macroscopic tumors.

Materials and methods

Animal maintenance and treatments

$Apc^{Min/+}$ mice were obtained from The Jackson Laboratory (Bar Harbor, ME). They were bred and maintained in a pathogen-free animal facility under standard 12:12 h light:dark cycle and fed on a basal diet, CE-2 (CLEA Japan, Tokyo, Japan), and water *ad libitum* until termination of the study (12,15).

Dextran sodium sulfate treatment

Dextran sodium sulfate (DSS) with a molecular weight of 36 000–50 000 (ICN Biochemicals) was dissolved in distilled water at a concentration of 2% (wt/vol). Eight male $Apc^{Min/+}$ mice were divided into experimental and control groups. The animals of experimental groups were administered 2% (wt/vol) DSS in drinking water for 1 week from 5 weeks of age. The dose was determined based on the results of previous studies (16).

β-Catenin/T-cell factor reporter transgenic mice, $Apc^{Min/+}$: β-catenin/T-cell factor reporter mice

For the generation of β-catenin/T-cell factor (Tcf) reporter mice, the Tcf-binding site and intron were polymerase chain reaction (PCR) amplified and cloned using a pTOPFLASH plasmid (Upstate Biotechnology, Lake Placid, NY) and CDM8 into a pEGFP-N3 plasmid (Clontech Japan, Tokyo, Japan) (3,17). The gene construct was excised from the vector and the fragment was microinjected into the pronuclei of fertilized C57BL/6 mouse eggs. Male β-catenin/Tcf reporter transgenic mice (strain C57BL/6) were bred with C57BL/6 females to produce transgenic mice on a C57BL/6 background. Genotyping was done using DNA extracted from tail biopsies of 3- to 4-week-old pups, and new breeding harems of 5- to 6-week-old mice were established to expand the β-catenin/Tcf reporter population before initiating separate crosses of the mice with the $Apc^{Min/+}$ mice. The offspring from these crosses yielded β-catenin/Tcf reporter $^{+/-}$:$Apc^{Min/+}$ mice.

Flow cytometry

Splenocytes of β-catenin/Tcf reporter mice were dissected and dissociated with phosphate-buffered saline (PBS). They were plated at a density of 10^6 cells/ml and maintained for 24 h in Dulbecco's modified Eagle's medium with 50 mmol/l LiCl, 50 mmol/l NaCl or H_2O only for controls (18,19). After 24 h,

the cells were washed and resuspended in PBS containing 3% fetal calf serum (staining medium). Cells were filtered through nylon mesh to remove large clumps, washed and resuspended in staining medium containing 0.5 μl/ml propidium iodide (Calbiochem-Novabiochem Corp., San Diego, CA) to eliminate dead cells. These cells were analyzed by FACS using a Vantage SE flow cytometer (Becton Dickinson, San Jose, CA) (20), and then the data were analyzed using CELLQuest software (Becton Dickinson). Gating was implemented based on wild-type litter mice as a negative control (data not shown).

Tumor analysis and tissue processing

Animals were killed and their colons were removed and cut open along their longitudinal axis. For paraffin sections, they were fixed flat in 10% buffered formalin for 24 h at room temperature, and for frozen sections, they were fixed in 4% buffered paraformaldehyde for 1 h at room temperature (12,14). Colon tumors that were macroscopically identified were divided into three groups. The first was fixed in 10% buffered formalin with the surrounding normal mucosa; the second was fixed in 4% buffered paraformaldehyde; and the third was snap frozen in liquid nitrogen, stored at −80°C and used for either DNA or RNA extraction (14,21).

Immunohistochemical analysis of tissue sections

Paraffin sections (4 μm) were treated with 0.01 M sodium citrate buffer (pH 6.0) four times in a microwave oven at high power for 6 min. They were treated with a methanol solution containing 5% H_2O_2 for 10 min, to block endogenous peroxidases. After blocking with 2% bovine serum albumin in PBS for 40 min at room temperature, they were treated with primary antibodies, anti-β-catenin (Transduction Laboratories, Lexington, KY; 1:1000), anti-enhanced green fluorescent protein antibody (Molecular Probes, Eugene, OR; 1:1000), anti-Myc N262 antibody (Santa Cruz Biotechnology, Santa Cruz, CA; 1:100) and anti-cyclin D1 antibody (Santa Cruz Biotechnology; 1:100) overnight at 4°C. For β-catenin staining, they were incubated with a tetramethyl rhodamine-conjugated secondary antibody (Jackson ImmunoResearch, West Grove, PA; 1:250) for 30 min, or for enhanced green fluorescent protein staining, they were incubated with fluorescein isothiocyanate-conjugated secondary antibody (Dakocytomation Japan, Kyoto, Japan; 1:250) for 30 min, before detection was done using a fluorescence microscope (Olympus Optical Co., Ltd., Tokyo, Japan) after 4′,6-diamidino-2-phenylindole (Nacalai Tesque, Kyoto, Japan) staining for 5 min (22). For cyclin D1 and Myc, the sections were incubated with a biotin-conjugated anti-rabbit secondary antibody (1:250) for 30 min and avidin conjugate of horseradish peroxidase for 30 min at room temperature (Vector Laboratories, Burlingame, CA; 1:250). Detection was done with 3,3-diaminobenzidine tetrahydrochloride (Dakocytomation Japan) for 0.5–10 min at room temperature and counterstained with hematoxylin (21). After blocking with 2% bovine serum albumin in PBS for 40 min at room temperature, they were incubated with the primary antibody, anti-mDkk1 antibody (R&D Systems, Minneapolis, MN; 1:100) overnight at 4°C. They were incubated with tetramethyl rhodamine-conjugated anti-rat secondary antibody for 30 min at room temperature. Detection was done using a fluorescence microscope after 4′,6-diamidino-2-phenylindole staining for 5 min. For β-catenin and GFP staining, digital images of microadenomas (n = 7), macroscopic tumors (n = 17) and the surrounding normal crypts were acquired using a fluorescence microscope (DP-70, Olympus Optical Co.). In the measurement of fluorescent intensities, the mean intensity of the whole nuclear area of a single cell in microadenomas, macroscopic tumors and their adjacent normal crypts was measured by an image-processing software program (NIH image). The average values of the nuclear fluorescent intensity in each crypts of two distinct lesions and adjacent control mucosa were calculated and the ratio of the value in each lesion to that in adjacent control crypts were compared by a statistical analysis using Mann–Whitney's U-test.

Real-time reverse transcription–polymerase chain reaction

Total RNA was isolated from snap-frozen tissues using the RNA queous-4PCR (Ambion, Austin, TX) according to the manufacturer's protocol. Up to 200 ng of total RNA was subjected to reverse transcription using Superscript III Reverse Transcriptase (Invitrogen Life Technologies, Carlsbad, CA). Real-time reverse transcription–polymerase chain reaction (RT–PCR) amplification was carried out in a final volume of 20 μl containing 10 μl of 2× SYBR green master mix (Takara, Kyoto, Japan), 1 μl of primers (10 μmol/l) and 5 μl of cDNA using a LightCycler 1.0. (Roche Diagnostics, Indianapolis, IN) according to the protocols described previously (21). The primers used in the present study are shown in supplementary Table 1, available at *Carcinogenesis* Online. Reaction conditions were activation at 95°C for 10 min, denaturation at 95°C for 10 s, annealing 60°C for 10 s and extension 72°C for 6 s. All PCR amplifications were done for 40 cycles and a melt curve analysis was used to examine the specificity of an amplified product. Standard curves were generated to quantify the expression levels of each target gene in comparison with the 18S rRNA or β-actin reference genes in each sample. The relative expression levels of each gene were calculated, dividing the value of these genes by those of the internal control genes (18S rRNA or β-actin).

Sodium bisulfite treatment and sequencing analysis

Genomic DNA from tumors and control mucosa were subjected to sodium bisulfite modification (EZ DNA Methylation-Gold Kit, Zymo Research, Orange, CA) as described previously (23). After PCR amplification using primers listed in supplementary Table 1, available at *Carcinogenesis* Online, the products were cloned into the TOPO vector. The inserted PCR fragments of the individual clones obtained from each sample were sequenced with both M13 reverse and M13 forward primers using the ABI Prism Dye Terminator Cycle Sequencing Kit and an ABI Prism 3100 DNA Sequencer.

Results

Two distinct stages in the colon of $Apc^{Min/+}$ mice

In order to verify the two-stage model of tumorigenesis in the colon of $Apc^{Min/+}$ mice, colonic mucosa of $Apc^{Min/+}$ mice at three different ages (5, 20 and 35 weeks) were examined in *en face* histological sections. The longest diameter of the intramucosal lesions that were hardly detectable in whole-mount preparations were measured on the histological sections of the mice at each of the investigated ages. The sizes of most intramucosal lesions remained within 300 μm and majority of microadenomas did not grow into a macroscopic tumor even at 35 weeks of age, thus suggesting that microadenomas are self-limiting lesions (Figure 1A). We further treated $Apc^{Min/+}$ mice with a potent tumor promoter, DSS in order to determine whether such microadenomas have a potential to progress into larger lesions and microadenomas are precursors of macroscopic lesions. Importantly, the size of microadenomas significantly increased by the DSS treatment, indicating that microadenomas started to grow by a well-known strong promoter of the tumorigenesis (Figure 1B). These findings represent two distinct stages of tumorigenesis in the colon of $Apc^{Min/+}$ mice.

Increased expression of β-catenin and its target genes in macroscopic tumors in the colon of $Apc^{Min/+}$ mice

Immunohistochemical analysis of β-catenin protein demonstrated that although microadenomas already revealed increased levels of nuclear β-catenin (n = 7), macroscopic tumors had further increased levels of nuclear β-catenin (n = 17) on the same slide of *en face* sections (Figure 2C and D). This was followed by a comparison of fluorescent signals of nuclear β-catenin. The results showed that the signal intensity of β-catenin in macroscopic tumors was higher than that of microadenomas (Figure 2E) ($P < 0.005$ by Mann–Whitney U-test). Immunostaining revealed that Myc and cyclin D1, well-known targets of β-catenin/Tcf transcription, were detectable in the nucleus of both microadenomas (n = 16) and macroscopic tumors (n = 15). However, the strong nuclear staining was observed only in macroscopic tumors (Figure 2F–I).

Reporter mice for β-catenin/Tcf transcriptional activity

In the present study, transgenic mice were generated with a reporter for β-catenin/Tcf transcriptional activity (Figure 3A). To confirm that the reporter mice actually represent transcriptional activity of β-catenin/Tcf signals *in vivo*, primary splenocytes of the transgenic mice were treated with LiCl, an inhibitor of GSK-3β and an activator of β-catenin/Tcf transcription. Flow cytometry revealed an increased GFP signal in the splenocytes with the LiCl treatment, suggesting that GFP reporter works *in vivo* (Figure 3B).

β-Catenin/Tcf transcriptional activity in two distinct stages of colon carcinogenesis

The mRNA expression for GFP in colon tumors and normal colonic mucosa in $Apc^{Min/+}$ mice with GFP reporter allele was analyzed by semiquantitative RT–PCR. The GFP expression in colon tumors (n = 12) was significantly higher than that in the normal colonic mucosa (n = 8, supplementary Figure 1, available at *Carcinogenesis*

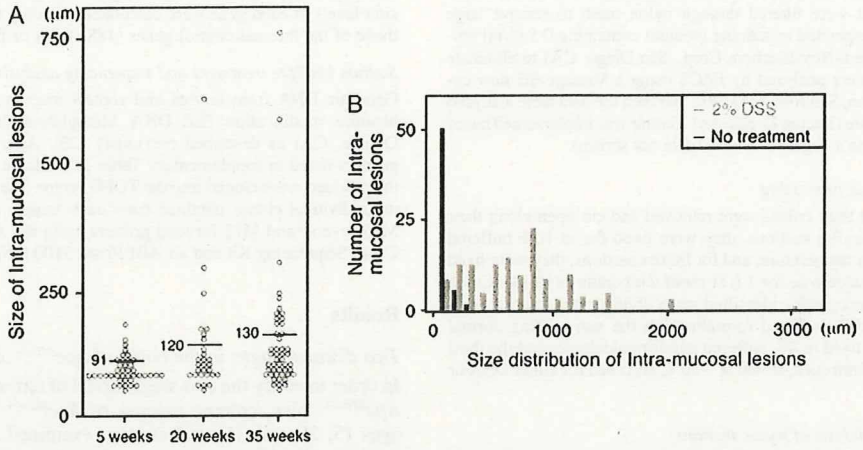

Fig. 1. Two distinct stages of tumorigenesis in the colon of $Apc^{Min/+}$ mice. (**A**) Size distribution of intramucosal lesions in the colon of $Apc^{Min/+}$ mice at 5, 20 and 35 weeks. The sizes of almost all intramucosal lesions remain <300 μm in their diameter and do not progress to a macroscopic tumor. Bars indicate average sizes of microadenomas. (**B**) DSS initiates the growth of microadenomas in the colon of $Apc^{Min/+}$ mice. The size distribution of the 'self-limiting' microadenomas increases by the treatment of DSS.

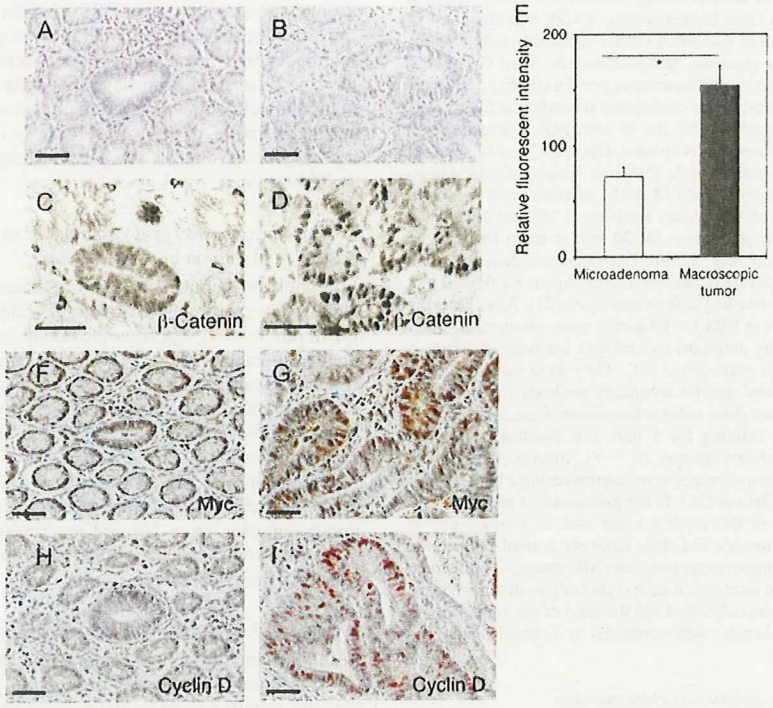

Fig. 2. Increased nuclear β-catenin and β-catenin/Tcf targets in colon tumor cells of $Apc^{Min/+}$ mice. (**A** and **B**) Histological appearance of microadenoma (A) and macroscopic tumor (B). Hematoxylin and eosin staining. Bars = 30 μm. (**C** and **D**) β-Catenin immunostaining of both lesions. Fluorescent intensities of nuclear β-catenin are higher in macroscopic tumor cells than those in microadenoma cells. Bars = 30 μm. (**E**) Measurement of fluorescent intensity of both lesions. The relative intensity of nuclear β-catenin staining is shown. $^{*}P < 0.005$ by Mann–Whitney *U*-test. (**F–I**) Myc and cyclin D1 immunostaining of both lesions. Nuclear staining of both Myc and cyclin D1 protein further increases in macroscopic tumor cells in comparison with microadenoma cells. Bars = 30 μm.

Online) ($P < 0.01$ by Mann–Whitney *U*-test). We next measured the fluorescence intensity of immunofluorescent staining of GFP at normal crypts, microadenomas and macroscopic tumors. The fluorescent signals in microadenomas have already increased when compared with those in adjacent normal crypts (Figure 3C and E) ($P < 0.005$ by Mann–Whitney *U*-test). However, GFP signals in macroscopic tumor were further upregulated in comparison with those in microadenomas (Figure 3C and H) ($P < 0.005$ by Mann–Whitney *U*-test). In this study, three different lines of transgenic mice were generated. GFP expression in all lines showed the same pattern, excluding the possibility that the observation depends on the locus in which transgenes were integrated.

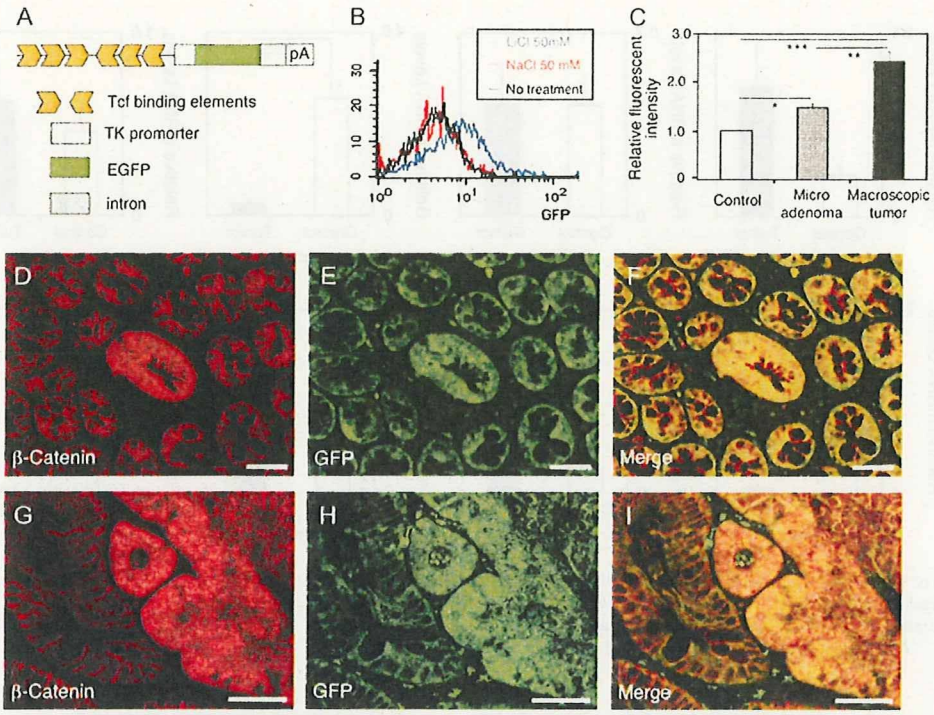

Fig. 3. β-Catenin/Tcf reporter mice. **(A)** Structure of the transgene. **(B)** β-Catenin/Tcf reporter works in the transgenic mice. LiCl, a Wnt signal activator, induces GFP expression in splenocytes of β-catenin/Tcf reporter transgenic mice. **(C)** Fluorescent signal of GFP stainings. GFP signal is higher in microadenomas in comparison with the surrounding normal crypts. Note that the reporter expression is significantly upregulated in macroscopic tumors when compared with microadenomas. $^{*}P < 0.005$, $^{**}P < 0.005$ and $^{***}P < 0.005$, by Mann–Whitney *U*-test. **(D–I)** GFP signals are detectable in both microadenomas and macroscopic tumors. Note that the strong GFP expression is observed only in macroscopic tumors. Bars = 30 μm.

Altered expressions of Wnt antagonist genes in colon tumors of $Apc^{Min/+}$ mice

Previous studies have shown that loss of Apc function and consequent accumulation of β-catenin occurs in the microadenomas, suggesting that the β-catenin/Tcf signaling pathway is already activated in the initiation stage (12). Wnt antagonist genes are epigenetically silenced in most human colorectal cancers (24–28), and such silencing has been shown to further increase the transcriptional activity of the β-catenin/Tcf signaling pathway, regardless of Apc inactivation (28–30). To investigate the involvement of Wnt antagonists in further upregulation of β-catenin/Tcf signaling in the macroscopic tumors of this model, mRNA levels for Wnt antagonist genes in macroscopic tumors and control mucosa were compared by semiquantitative real-time RT–PCR. The Wnt antagonist genes examined in the present study were *Sfrp1*, *Sfrp2*, *Sfrp4*, *Sfrp5*, *Dkk1*, *Dkk2*, *Dkk3* and *Dkk4*. *Sfrp4*, *Dkk1* and *Dkk4* expression was significantly decreased in macroscopic tumors in comparison with control mucosa (Figure 4) ($P < 0.05$, $P < 0.001$ and $P < 0.001$, respectively, by Mann–Whitney *U*-test). In contrast, *Dkk2* expression was significantly increased in macroscopic tumors (Figure 4) ($P < 0.05$ by Mann–Whitney *U*-test).

Dkk1 expression in two distinct stages of colon tumorigenesis

Among three Wnt antagonist genes (*Sfrp4*, *Dkk1* and *Dkk4*) that are downregulated in macroscopic tumors, only Dkk1 is shown to have the ability to functionally suppress β-catenin/Tcf transcription in the intestine of mice (29,30). Additionally, it is interesting to note that decreased *Dkk1* expression is frequently observed in human colon cancers (26,28). Therefore, the Dkk1 expression was examined in two distinct lesions by immunostaining to determine when the Dkk1 expression decreased in the course of multistage carcinogenesis in the colon of $Apc^{Min/+}$ mice. Consistent with the results in the RT–PCR analysis, decreased fluorescent intensities of Dkk1 were observed in macroscopic tumors in comparison with those in the surrounding control mucosa (5/8) (Figure 5). This was consistent with the previous RT–PCR results. In contrast, the Dkk1 expression in microadenoma is higher than that of the surrounded control mucosa (6/6) (Figure 5). These results suggest that Dkk1 expression is decreased in the course of the transition from microadenomas to macroscopic tumors.

Methylation status of Dkk1 and Sfrp4 promoter regions in colon tumors of $Apc^{Min/+}$ mice

Epigenetic silencing of Wnt antagonist genes in human colon cancers is often accompanied by DNA hypermethylation (24,30). Since mouse *Dkk4* has no apparent clustering of CpG sites in the promoter region, the methylation status of *Dkk1* and *Sfrp4* promoters was examined by bisulfite sequencing. The promoter region of *Dkk1* (27 clones from three colons) and *Sfrp4* (nine clones from two colons) was unmethylated in the control mucosa. However, no evidence of DNA hypermethylation was detected in colon tumors in the *Dkk1* (28 clones from three colon tumors) and *Sfrp4* (6 clones from two colon tumors) promoters, regardless of the mRNA expression status (Figure 6).

Discussion

Colorectal tumors progress through a series of clinical and histopathological stages, ranging from single crypt lesions to invasive cancers (2). Accumulating evidence suggests that such progression results from a series of genetic and epigenetic changes (2,31). However, how such alterations are linked to the histopathological progression is not fully understood. A previous study has shown that two lesions, microadenomas and macroscopic tumors, are distinguishable in the colon of $Apc^{Min/+}$ mice (12). In this study, we have shown that

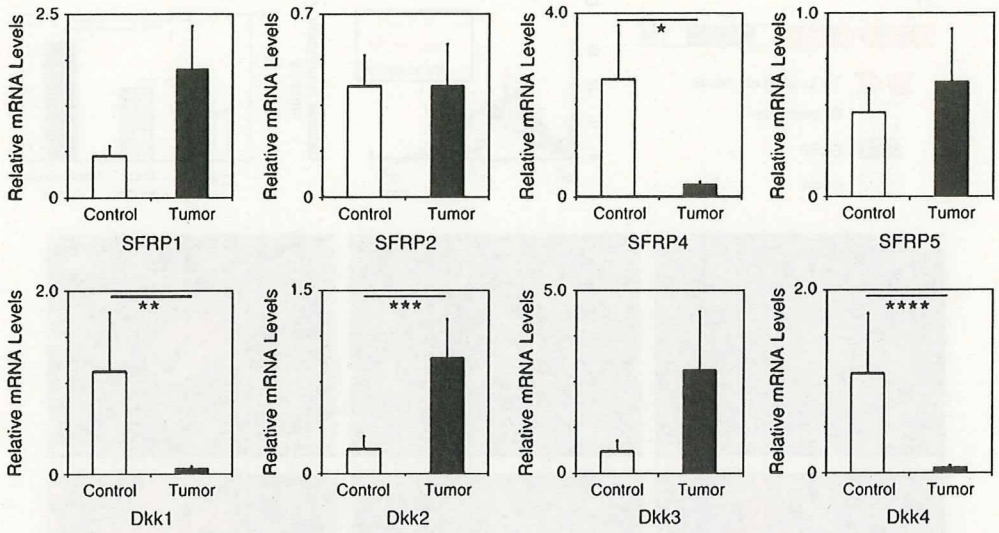

Fig. 4. Expression of Wnt antagonist genes in colon tumors of $Apc^{Min/+}$ mice was assessed by semiquantitative real-time RT–PCR. The expression of *Sfrp4*, *Dkk1* and *Dkk4* was upregulated, whereas the expression of *Dkk2* was downregulated. The expression was normalized to S18 or β-actin mRNA expression. Samples were analyzed in triplicate. (Columns, mean of three independent experiments; bars, SEM; $n = 12$ for tumor and $n = 8$ for control. $^{*}P < 0.05$, $^{**}P < 0.001$, $^{***}P < 0.05$ and $^{****}P < 0.001$; by Mann–Whitney *U*-test.)

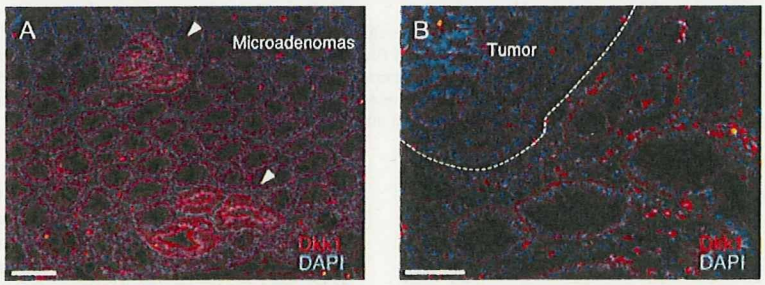

C

	Microadenoma	Macroscopic tumor
Expression level		
high	6	0
equal	0	3
low	0	5

Fig. 5. Immunohistochemistry of Dkk1 in microadenomas and macroscopic tumors in the colon of $Apc^{Min/+}$ mice. (**A** and **B**) Fluorescent signal levels decrease in the macroscopic tumor. Note that Dkk1 is upregulated in microadenomas. Bars = 30 μm. (**C**) Summary of Dkk1 staining in two lesions.

microadenomas themselves are self-limiting lesions, but such microadenomas can potentially grow into larger lesions by inflammatory stimuli. Together with previous lines of experiments, these findings indicate the existence of two stages of tumorigenesis in the colon of $Apc^{Min/+}$ mice and suggest that additional stochastic alterations are required for microadenomas to progress into macroscopic tumors. Although the loss of the *Apc* function through LOH is associated with the initial microadenoma formation (12), the underlying mechanism of the development of macroscopic tumors remained elusive. A previous study using a rat model for colon cancer demonstrated that intramucosal lesions possess a wide spectrum of mutations in the β-catenin gene, but only lesions with specific mutations that directly regulate β-catenin levels developed macroscopic tumors (32). Based on those findings, it is assumed that sufficient β-catenin accumulation may be required for the development of macroscopic tumors. The present study showed that the nuclear accumulation of β-catenin and the expression of Myc and cyclin D1, well-known downstream targets of the β-catenin/Tcf signaling pathway, were significantly upregulated in macroscopic tumors when compared with microadenomas. Using β-catenin/Tcf reporter mice, the β-catenin/Tcf transcriptional activity was measured directly as the amount of GFP *in vivo*. This demonstrated an increased GFP expression in macroscopic tumors in comparison with that in microadenomas. These results suggest that further activation of the β-catenin/Tcf signaling activity might be responsible for the development of macroscopic tumors from microadenomas. Although significant evidence suggests that the activation of β-catenin signaling is an initiating event in the colon tumorigenesis, the present findings may shed light on the role of β-catenin/Tcf transcription on the later stage of the tumorigenesis. There may be a threshold of β-catenin/Tcf transcriptional activity when small lesions

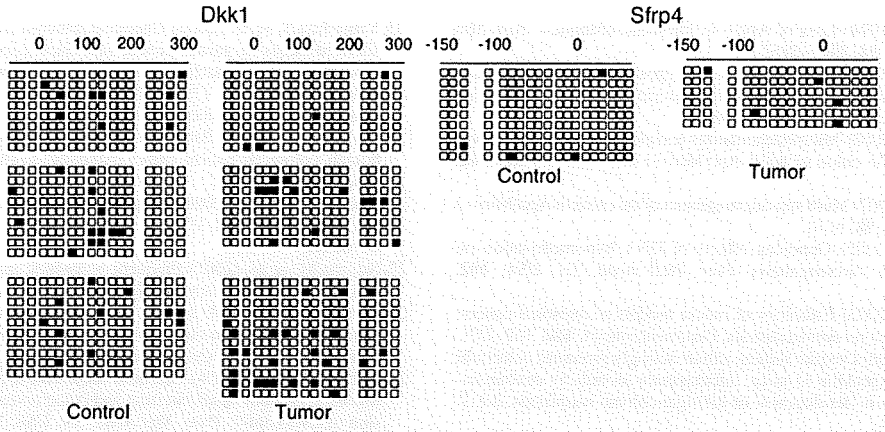

Fig. 6. Results of bisulfite DNA sequencing of the promoter CpG island region of *Dkk1* and *Sfrp4*. Numbers represent the positions relative to the transcription start site. Square, CpG dinucleotide (potential target of methylation); closed square, methylated CpG dinucleotide and open square, unmethylated CpG dinucleotide.

progress into macroscopic tumors, and only lesions that exceed that threshold could grow into a macroscopic lesion.

A recent study indicated that β-catenin/Tcf signaling in colon cancer cells could be further activated by upstream signals regardless of the constitutive activation of the pathway by downstream mutations (30). The present study showed altered expression of a number of Wnt antagonist genes in the colon tumors of $Apc^{Min/+}$ mice. Importantly, although the level of Dkk1 protein was decreased in most macroscopic tumors, Dkk1 expression in microadenomas was increased in comparison with the adjacent normal mucosa. This study suggests that the decreased levels of Dkk1 play a role in further activation of β-catenin/Tcf transcription. Detailed analyses are necessary to elucidate the functional significance of the decreased Dkk1 on the β-catenin/Tcf transcription in colon tumors of $Apc^{Min/+}$ mice.

The present findings also raised additional questions of the underlying mechanism that induces the silencing of Dkk1 in macroscopic tumors. Recently, epigenetic inactivation of Wnt antagonist genes has been reported in most human colorectal cancers (26). In addition, mice deficient DNA methyltransferases have been shown to block the development of macroscopic tumors in the colon of $Apc^{Min/+}$mice (14,33), suggesting that DNA methylation plays a role in the development of macroscopic tumors. In order to determine whether the inactivation of Wnt antagonist genes is associated with DNA hypermethylation, the methylation status of the promoter region of *Dkk1* and *Sfrp4*, which were silenced in colon tumors of $Apc^{Min/+}$ mouse model, was investigated. However, no significant difference in the DNA methylation status between macroscopic tumors and control mucosa was detectable, thus suggesting that *Dkk1* downregulation is independent of DNA hypermethylation. Accordingly, it is possible that other epigenetic silencing, such as histone modifications may be associated with the inactivation and this might provide a useful model to study the epigenetic silencing that is independent of DNA hypermethylation in these tumors.

Although the fact that most microadenomas have the ability to progress into macroscopic tumors supports the idea that macroscopic tumors arise from a subset of microadenomas, we cannot exclude a possibility that there are alternative pathways in which normal colon epithelium is converted into macroscopic tumor cells. Indeed, recent evidences strongly suggest that histological changes are preceded by epigenetic alterations that are associated with the activation of β-catenin/Tcf transcription in the colon (30,34). Meanwhile, it is also possible that microadenomas and macroadenomas may originate from different cell types in terms of the differentiation state. Therefore, small adenomatous lesions may not be uniform lesions and such differences might affect the later progression; thus, some microadenomas may more easily progress into macroscopic tumors than others. Further investigations are required to elucidate the multiple genetic and/or epigenetic pathways of tumor development in the colon.

In summary, these findings suggest that activation of β-catenin/Tcf transcription, which is accompanied by an increased nuclear β-catenin level and decreased Dkk1 expression, plays a role in the development of macroscopic tumors in the colon of $Apc^{Min/+}$ mice. In addition, the β-catenin/Tcf reporter transgenic mice described here would be useful to elucidate the biological role of β-catenin/Tcf transcription *in vivo*.

Supplementary material

Supplementary Figure 1 and Table 1 can be found at http://carcin.oxfordjournals.org/

Funding

Ministry of Health, Labour and Welfare of Japan; The Ministry of Education, Culture, Sports, Science and Technology of Japan.

Acknowledgements

We thank Dr Toshikazu Ushijima for helpful comments and critical reading of the manuscript. We also thank Kyoko Takahashi, Ayako Suga and Yoshitaka Kinjyo for the technical assistance and the animal care.

Conflict of Interest Statement: None declared.

References

1. Vogelstein,B. *et al.* (1988) Genetic alterations during colorectal-tumor development. *N. Engl. J. Med.*, **319**, 525–532.
2. Fearon,E.R. *et al.* (1990) A genetic model for colorectal tumorigenesis. *Cell*, **61**, 759–767.
3. Morin,P.J. *et al.* (1997) Activation of beta-catenin-Tcf signaling in colon cancer by mutations in beta-catenin or APC. *Science*, **275**, 1787–1790.
4. Powell,S.M. *et al.* (1992) APC mutations occur early during colorectal tumorigenesis. *Nature*, **359**, 235–237.
5. Groden,J. *et al.* (1991) Identification and characterization of the familial adenomatous polyposis coli gene. *Cell*, **66**, 589–600.
6. Nishisho,I. *et al.* (1991) Mutations of chromosome 5q21 genes in FAP and colorectal cancer patients. *Science*, **253**, 665–669.
7. Moser,A.R. *et al.* (1990) A dominant mutation that predisposes to multiple intestinal neoplasia in the mouse. *Science*, **247**, 322–324.
8. Su,L.K. *et al.* (1992) Multiple intestinal neoplasia caused by a mutation in the murine homolog of the APC gene. *Science*, **256**, 668–670.
9. Levy,D.B. *et al.* (1994) Inactivation of both APC alleles in human and mouse tumors. *Cancer Res.*, **54**, 5953–5958.

10. Luongo,C. *et al.* (1994) Loss of Apc+ in intestinal adenomas from Min mice. *Cancer Res.*, **54**, 5947–5952.
11. Oshima,M. *et al.* (1995) Loss of Apc heterozygosity and abnormal tissue building in nascent intestinal polyps in mice carrying a truncated Apc gene. *Proc. Natl Acad. Sci. USA*, **92**, 4482–4486.
12. Yamada,Y. *et al.* (2002) Microadenomatous lesions involving loss of Apc heterozygosity in the colon of adult Apc(Min/+) mice. *Cancer Res.*, **62**, 6367–6370.
13. Yamada,Y. *et al.* (2007) Multistep carcinogenesis of the colon in Apc(Min/+) mouse. *Cancer Sci.*, **98**, 6–10.
14. Yamada,Y. *et al.* (2005) Opposing effects of DNA hypomethylation on intestinal and liver carcinogenesis. *Proc. Natl Acad. Sci. USA*, **102**, 13580–13585.
15. Boivin,G.P. *et al.* (2003) Pathology of mouse models of intestinal cancer: consensus report and recommendations. *Gastroenterology*, **124**, 762–777.
16. Tanaka,T. *et al.* (2006) Dextran sodium sulfate strongly promotes colorectal carcinogenesis in Apc(Min/+) mice: inflammatory stimuli by dextran sodium sulfate results in development of multiple colonic neoplasms. *Int. J. Cancer*, **118**, 25–34.
17. Korinek,V. *et al.* (1997) Constitutive transcriptional activation by a beta-catenin-Tcf complex in APC-/- colon carcinoma. *Science*, **275**, 1784–1787.
18. Stambolic,V. *et al.* (1996) Lithium inhibits glycogen synthase kinase-3 activity and mimics wingless signalling in intact cells. *Curr. Biol.*, **6**, 1664–1668.
19. Klein,P.S. *et al.* (1996) A molecular mechanism for the effect of lithium on development. *Proc. Natl Acad. Sci. USA*, **93**, 8455–8459.
20. Walker,P.R. *et al.* (1991) Topoisomerase II-reactive chemotherapeutic drugs induce apoptosis in thymocytes. *Cancer Res.*, **51**, 1078–1085.
21. Tomita,H. *et al.* (2007) Development of gastric tumors in Apc(Min/+) mice by the activation of the beta-catenin/Tcf signaling pathway. *Cancer Res.*, **67**, 4079–4087.
22. Yamada,Y. *et al.* (2003) Pre-cancerous lesions for colorectal cancers in rodents: a new concept. *Carcinogenesis*, **24**, 1015–1019.
23. Yamashita,S. *et al.* (2006) Chemical genomic screening for methylation-silenced genes in gastric cancer cell lines using 5-aza-2′-deoxycytidine treatment and oligonucleotide microarray. *Cancer Sci.*, **97**, 64–71.
24. Caldwell,G.M. *et al.* (2004) The Wnt antagonist sFRP1 in colorectal tumorigenesis. *Cancer Res.*, **64**, 883–888.
25. He,B. *et al.* (2005) Blockade of Wnt-1 signaling induces apoptosis in human colorectal cancer cells containing downstream mutations. *Oncogene*, **24**, 3054–3058.
26. Aguilera,O. *et al.* (2006) Epigenetic inactivation of the Wnt antagonist DICKKOPF-1 (DKK-1) gene in human colorectal cancer. *Oncogene*, **25**, 4116–4121.
27. Nojima,M. *et al.* (2007) Frequent epigenetic inactivation of SFRP genes and constitutive activation of Wnt signaling in gastric cancer. *Oncogene*.
28. Gonzalez-Sancho,J.M. *et al.* (2005) The Wnt antagonist DICKKOPF-1 gene is a downstream target of beta-catenin/TCF and is downregulated in human colon cancer. *Oncogene*, **24**, 1098–1103.
29. Kuhnert,F. *et al.* (2004) Essential requirement for Wnt signaling in proliferation of adult small intestine and colon revealed by adenoviral expression of Dickkopf-1. *Proc. Natl Acad. Sci. USA*, **101**, 266–271.
30. Suzuki,H. *et al.* (2004) Epigenetic inactivation of SFRP genes allows constitutive WNT signaling in colorectal cancer. *Nat. Genet.*, **36**, 417–422.
31. Jones,P.A. *et al.* (2002) The fundamental role of epigenetic events in cancer. *Nat. Rev. Genet.*, **3**, 415–428.
32. Yamada,Y. *et al.* (2003) Beta-catenin mutation is selected during malignant transformation in colon carcinogenesis. *Carcinogenesis*, **24**, 91–97.
33. Lin,H. *et al.* (2006) Suppression of intestinal neoplasia by deletion of Dnmt3b. *Mol. Cell. Biol.*, **26**, 2976–2983.
34. Linhart,H.G. *et al.* (2007) Dnmt3b promotes tumorigenesis *in vivo* by gene-specific de novo methylation and transcriptional silencing. *Genes. Dev.*, **21**, 3110–3122.

Received July 11, 2007; revised December 16, 2007; accepted December 28, 2007

Int. J. Cancer: **121,** 301–307 (2007)

Silencing of tissue factor pathway inhibitor-2 gene in malignant melanomas

Yoshimasa Nobeyama[1,2], Eriko Okochi-Takada[1], Junichi Furuta[1,3], Yohei Miyagi[4], Kanako Kikuchi[5], Akifumi Yamamoto[6], Yukihiro Nakanishi[7], Hidemi Nakagawa[2] and Toshikazu Ushijima[1]*

[1]*Carcinogenesis Division, National Cancer Center Research Institute, 5-1-1 Tsukiji, Chuo-ku, Tokyo, Japan*
[2]*Department of Dermatology, The Jikei University School of Medicine, 25-8-3, Nishishimbashi, Minato-ku, Tokyo, Japan*
[3]*Department of Dermatology, Graduate School of Comprehensive Human Sciences, University of Tsukuba, 1-1-1 Ten-noudai, Tsukuba, Ibaraki, Japan*
[4]*Molecular Pathology and Genetics, Kanagawa Cancer Center Research Institute, 1-1-2 Nakao, Asahi-ku, Yokohama, Japan*
[5]*Department of Dermatology, Faculty of Medicine, The University of Tokyo, 7-3-1 Hongo, Bunkyo-ku, Tokyo, Japan*
[6]*Dermatology Division, National Cancer Center Hospital, 5-1-1 Tsukiji, Chuo-ku, Tokyo, Japan*
[7]*Pathology Division, National Cancer Center Research Institute, 5-1-1 Tsukiji, Chuo-ku, Tokyo, Japan*

To identify tumor-suppressor genes inactivated by aberrant methylation of promoter CpG islands (CGIs) in human malignant melanomas, genes upregulated by treatment of cells with a demethylating agent, 5-aza-2′-deoxycytidine (5-aza-dC), were searched for using oligonucleotide microarrays in melanoma cell lines, HMV-I, MeWo and WM-115. Seventy-nine known genes with CGIs were identified as being upregulated (≥16-fold), and 18 of them had methylation of their putative promoter CGIs in 1 or more of 8 melanoma cell lines. Among the 18 genes, *TFPI-2*, which is involved in repression of the invasive potential of malignant melanomas, was further analyzed. Its expression was repressed in a melanoma cell line with its complete methylation, and was restored by 5-aza-dC treatment. It was unmethylated in cultured neonatal normal epidermal melanocyte, and was induced by ultraviolet B. In surgical melanoma specimens, *TFPI-2* methylation was detected in 5 of 17 metastatic site specimens (29%), while it was not detected in 20 primary site specimens (0%) ($p = 0.009$). By immunohistochemistry, the 5 specimens with promoter methylation lacked immunoreactivity for TFPI-2. The results showed that *TFPI-2* is silenced in human malignant melanomas by methylation of its promoter CGI and suggested that its silencing is involved in melanoma metastasis.

Key words: TFPI-2; silencing; DNA methylation; malignant melanoma; oligonucleotide microarray

The incidence of malignant melanoma has been steadily increasing in Western countries over the past few decades.[1] It is one of the tumors with the worst prognosis for its tendency to metastasize and its resistance to conventional chemotherapy in advanced stages. Although it is recognized that therapies based on specific molecular targets can be very effective for some cancers,[2,3] the molecular pathogenesis of malignant melanomas has only been partially elucidated. Known genetic alterations include mutational activations of *N-ras* (5–37.5%)[4,5] and *B-RAF* (80%),[6] and inactivations of *CDKN2A* (11–44%)[7,8] and *PTEN* (14%)[9] by chromosomal deletions. On the other hand, contrary to the initial expectation that epigenetic aberrations would be infrequent in malignant melanomas, increasing numbers of genes are shown to be inactivated by methylations of their promoter CpG islands (CGIs), including *CDKN2A* (32%),[10] *RASSF1A* (41–50%),[11] *TIMP3*,[12] *PRDX2* (8%)[13] and *TSPY* (5/5 in males).[14]

Genome-wide screening for aberrant methylation is useful to identify genes with epigenetic aberrations, and various techniques have been developed.[15] Most techniques are based on the methylation status of genomic DNA, including methylation-sensitive-representational difference analysis (MS-RDA) and restriction landmark genomic scanning.[15] We previously applied MS-RDA to 3 melanoma cell lines, MeWo, WM-266-4 and MMAc, and identified silencing of *PRDX2*,[13] a negative regulator of PDGF signaling.[16] Another technique developed by Suzuki *et al.* utilizes a demethylating agent, 5-aza-2′-deoxycytidine (5-aza-dC), and a microarray to identify genes reexpressed by demethylation.[17] This chemical genomic screening is simple and effective in identifying genes silenced in cell lines.[18] Since only a minor fraction of tumor-related genes are finally utilized as molecular targets, we need to determine more genes involved in melanomas, and chemical genomic screening is a choice.

In the present study, we performed a chemical genomic screening using 3 human melanoma cell lines, HMV-I, MeWo and WM-115. These cell lines were selected because they had different origins and frequencies of methylation[19]: HMV-I, MeWo and WM-115 originated from a primary lesion of genital mucosa, a metastatic lesion of a lymph node, and a primary skin lesion, respectively, and exhibited frequent, infrequent and intermediately frequent gene silencing, respectively.

Material and methods

Cell lines, tumor samples and nucleic acid extraction

Human melanoma cell lines, MeWo, VMRC-MELG, A2058, C32TG and GAK were obtained from the Health Science Research Resources Bank (Sennan, Japan); G361, SK-Mel-28 and HMV-I from the Cell Resource Center for Biomedical Research Institute of Development (Sendai, Japan); COLO 679 and MMAc from RIKEN BioResource Center (Tsukuba, Japan); WM-266-4 and WM-115 from the American Type Culture Collection (Rockville, MD) and cultured normal human epidermal melanocyte (HEM) from Cascade Biologics (Portland, OR).

Thirty-seven surgical melanoma specimens, 20 from primary sites and 17 from metastatic sites, were obtained from 37 patients in Stages III and IV determined by the American Joint Committee on Cancer with informed consents at Tsukuba University Hospital and The University of Tokyo Hospital. Thirty-three specimens were fixed in formalin and embedded in paraffin and 4 (Cases 6, 7, 32, 33) were fresh-frozen. Five lymph nodes specimens were obtained from 5 nonmelanoma skin cancer cases. For DNA extraction from paraffin-embedded melanoma specimens, specimens were sliced into 40-μm-thick tissue sections, deparaffinized and then dissected by a fine needle. After incubation in a lysis buffer (50 mM Tris-HCl, pH 8.5, 1 mM EDTA, 0.5% Tween-20, 200 mg/ml of proteinase K) at 55°C over night, DNA was extracted by the phenol/chloroform procedure. From cultured cells and fresh-

This article contains supplementary material available via the Internet at http://www.interscience.wiley.com/jpages/0020-7136/suppmat.

Grant sponsor: Ministry of Health, Labor and Welfare; Ministry of Education, Culture, Sports, Science and Technology, Japan.

***Correspondence to:** Carcinogenesis Division, National Cancer Center Research Institute, 5-1-1 Tsukiji, Chuo-ku, Tokyo 104-0045, Japan.
E-mail: tushijim@ncc.go.jp

Received 1 August 2006; Accepted after revision 16 January 2007
DOI 10.1002/ijc.22637
Published online 19 March 2007 in Wiley InterScience (www.interscience.wiley.com).

TABLE I – LIST OF GENES WHOSE PROMOTER CpG ISLANDS WERE METHYLATED IN MELANOMA CELL LINES

Number	Gene	Description	Accession number	Chromosomal location	Region analyzed by MSP	Methylation incidence
1	*ADFP*	adipose differentiation-related protein	NM_001122	9p21	19917683-804[1]	1/8
2	*ANGPTL4*	angiopoietin-like 4	NM_139314	19p13.3	8334705-842	2/8
3	*APM2*	adipose specific 2	NM_006829	10q23.2	88718121-207	5/8
4	*CLDN3*	claudin 3	NM_001306	7q11.23	72822580-716[1]	2/8
5	*F2RL1*	coagulation factor II (thrombin) receptor-like 1	NM_005242	5q13	7615463-583	1/8
6	*FKBP1B*	FK506 binding protein 1B	NM_004116	2p23.3	24125969-6063	1/8
7	*GREM1*	gremlin 1 homolog, cysteine knot superfamily	NM_013372	15q13-q15	30797292-442	1/8
8	*GSTM4*	glutathione S-transferase M4	NM_147148	1p13.3	110000074-223	1/8
9	*IRX4*	iroquois homeobox protein 4	NM_016358	5p15.3	1935993-6112[1]	1/8
10	*ISYNA1*	myo-inositol 1-phosphate synthase A1	NM_016368	19p13.11	18410001-168[1]	1/8
11	*MT1K*	metallothionein 1K	NM_005950	16q13	55259557-678[1]	3/8
12	*PDLIM4*	PDZ and LIM domain 4	NM_003687	5q31.1	131621019-118	4/8
13	*RRAD*	Ras-related associated with diabetes	NM_004165	16q22	65516994-7100[1]	2/8
14	*SPINT2*	serine protease inhibitor, Kunitz type, 2	NM_021102	19q13.1	43446926-7042	2/8
15	*TAC1*	tachykinin, precursor 1	NM_003182	7q21-q22	97199101-201	6/8
16	*TFPI-2*	tissue factor pathway inhibitor 2	NM_006528	7q22	93358033-228[1,2]	1/8
17	*TPM2*	tropomyosin 2 (beta)	NM_213674	9p13.2-p13.1	35680034-298[1]	2/8
18	*WARP*	von Willebrand factor A domain-related protein	NM_022834	1p36.33	1360665-798	2/8

[1]Positions in the reverse strand.–[2]Region analyzed by the new set of primers, which is shown as "MSP 2 in Figure 1*a*."

frozen specimens, DNA was extracted by the phenol/chloroform procedure or a QuickGene DNA tissue kit S (FUJIFILM, Tokyo, Japan). Total RNA was extracted from the cultured cells using ISOGEN (NIPPON GENE, Tokyo, Japan).

Treatment with 5-aza-2′-deoxycytidine and ultraviolet-B irradiation

For 5-aza-2′-deoxycytidine (5-aza-dC) treatment, melanoma cells were seeded at a density of 2×10^5–6×10^5 cells/10-cm dish on day 0 in RPMI 1640 (Invitrogen, Carlsbad, CA), exposed to a medium containing 1 μM 5-aza-dC (Sigma-Aldrich, St Louis, MO) for 48 hr on days 1 and 3 and harvested on day 5. All cell lines showed mild growth suppression on day 5, compared to untreated cells. Growth curve of HMV-I cells and their morphology after 5-aza-dC treatment are shown in Supplementary Figure 1.

For ultraviolet-B (UVB) irradiation, HEM was seeded at a density of 1.5×10^6 cells/10-cm dish on day 0 in Medium 254 (Cascade Biologics, Mansfield, UK), irradiated at doses of 0, 10 and 20 mJ/cm^2 on day 1 and harvested on day 2. HEMs were irradiated uncovered in phosphate-buffered saline (PBS) to UV generated by TL20W/12 tubes (Philip, Eindhoven, the Netherlands) at 0.51 mW/cm^2, monitored by a UV radiometer (Model UVR 3036/S2, Topcon, Tokyo, Japan).

Oligonucleotide microarray analysis

Oligonucleotide microarray analysis was performed using GeneChip Human Genome 133 Plus 2.0 (Affymetrix, Santa Clara, CA) with 54,000 probe sets, 47,400 transcripts from 39,000 genes. From 7 μg of total RNA, double-stranded cDNA was synthesized and biotin-labeled cRNA was prepared using a BioArray High-Yield RNA transcript labeling kit (Enzo, Farmingdale, NY). Twenty microgram of labeled cRNA was fragmented, and hybridized to GeneChips. Hybridization signals were scanned, processed using GeneChip Operating Software and normalized so that the average of all the genes on a GeneChip was 500. The *p*-values for differential expression (Change *p*-value) were calculated in each probe by statistical algorithms based on the Wilcoxon Signed-Rank test. The "Change *p*-values" of 0.003 and 0.997, respectively, were used as thresholds to define genes with increased and decreased expression.

Methylation-specific PCR and bisulfite sequencing

DNA samples (500 ng each) digested by *Bam*HI were denatured in 0.3 N NaOH at 37°C for 15 min. The samples in 3.6 N sodium bisulfite (pH 5.0) and 0.6 mM hydroquinone underwent 15 cycles of 30-sec denaturation at 95°C and 15-min incubation at 50°C. They were desalted with the Wizard DNA Clean-Up system (Promega, Madison, WI), and desulfonated in 0.3 N NaOH. DNA was ethanol-precipitated and dissolved in 20 μl of TE buffer.

Methylation-specific PCR (MSP) was performed with a primer set specific to the methylated or unmethylated sequence (M or U set), using 1 μl of the sodium bisulfite-treated DNA. Primers were designed in the 5′ regions of the reported transcription initiation site of candidate genes (Supplementary Table I). DNA methylated with *Sss*I methylase (New England Biolabs, Beverly, MA) and DNA amplified by GenomiPhi DNA amplification kit (GE Healthcare, Little Chalfont, UK) were used to determine specifically amplified conditions for M and U sets.[20] Minimum cycles to obtain visible bands with positive control samples were determined for each primer set and 4 cycles were added for test samples. A further 4 cycles were added for paraffin-embedded samples that were degraded.

For bisulfite sequencing, 1 μl of the sodium bisulfite-treated DNA was used for PCR with the primers common to methylated and unmethylated DNA sequences (Supplementary Table I). The PCR products were cloned into a pCR4-TOPO cloning vector (Invitrogen) and 10 clones or more were cycle-sequenced for each sample.

Quantitative real-time reverse transcription-PCR

Total RNA was treated with DNase I (Ambion, Austin, TX), and cDNA was synthesized from 1 μg of total RNA using a Superscript II kit (Life Technologies, Rockville, MD). Quantitative real-time reverse transcription-PCR (RT-PCR) was performed with the SYBR Green PCR Master Mix (Toyobo, Osaka, Japan) and a 7,300 Real Time PCR Systems (Applied Biosystems, Foster City, CA). The number of molecules of a specific gene in a sample was measured by comparing its amplification with that of standard samples, which contained 10^1 to 10^8 copies of the gene. The mRNA quantity of each gene was normalized with that of glyceraldehyde-3-phosphate dehydrogenase (*GAPDH*). The primers and PCR conditions are shown in Supplementary Table II.

Immunohistochemical analysis

Immunohistochemical staining of TFPI-2 was performed using a mouse monoclonal antibody against human TFPI-2 (clone 28Aa) as the primary antibody.[21] Formalin-fixed and paraffin-embedded sections were sliced at 4 μm thickness, deparaffinized and heated in 10 mM citrate buffer (pH 6.0) for 20 min at 95°C. After blocking, the sections were incubated with the primary antibody at a dilution of 100-fold at 4°C for 1 hr, and then with the second anti-

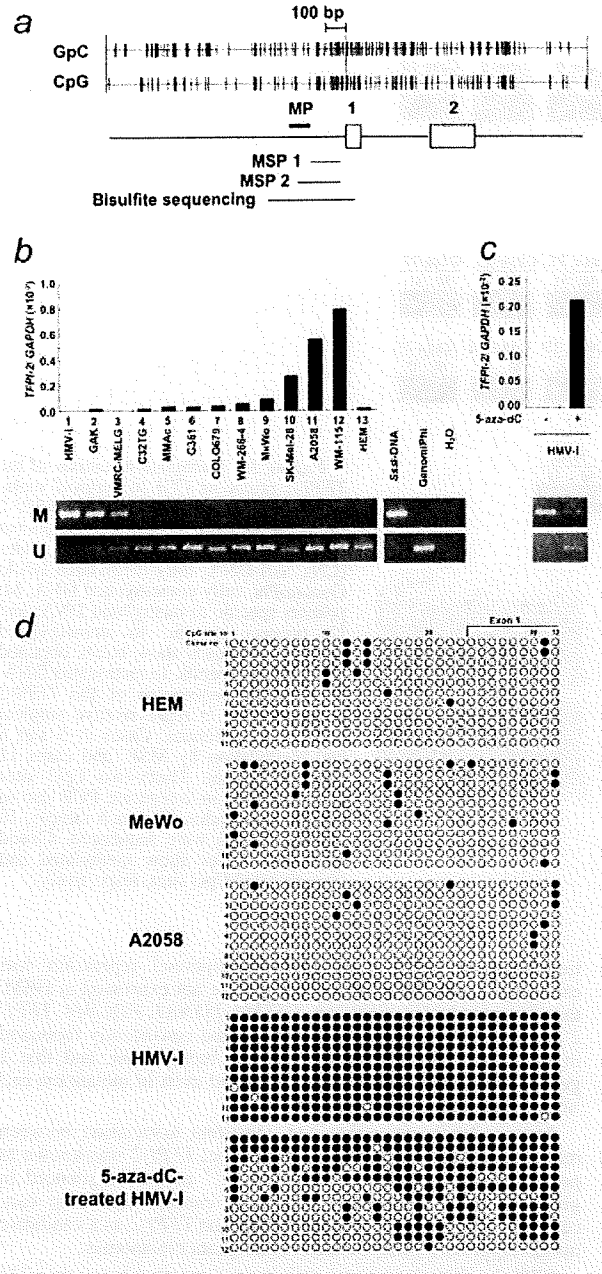

FIGURE 1 – (a) The genomic structure of *TFPI-2* in its promoter region. Vertical ticks show individual GpC sites (top) and CpG sites (bottom). The regions shown are those analyzed by the initial MSP (MSP 1), the second MSP (MSP 2) and the bisulfite sequencing. MP: minimal promoter region. (*b*) *TFPI-2* expression and methylation of its promoter CGI. *TFPI-2* expression and methylation were analyzed by quantitative RT-PCR and MSP, respectively, in 12 melanoma cell lines (Lanes 1–12) and HEM (Lane 13). M, primers specific to methylated DNA; U, primers specific to unmethylated DNA. As control fully methylated and fully unmethylated DNA, genomic DNA methylated using *Sss*I-methylase and genomic DNA amplified using phi29 DNA polymerase (GenomiPhi DNA), respectively, were used. HMV-I did not have unmethylated DNA molecules, and lacked *TFPI-2* expression. (*c*) *TFPI-2* reexpression after 5-aza-dC treatment was confirmed by quantitative RT-PCR. (*d*) Methylation of the *TFPI-2* promoter CGI shown by bisulfite sequencing. Thirty-two CpG sites were analyzed in HEM, MeWo, A2058, HMV-I, and HMV-I after 5-aza-dC treatment. For each sample, 10 or more clones were sequenced. Closed and open circles show methylated and unmethylated CpG sites, respectively.

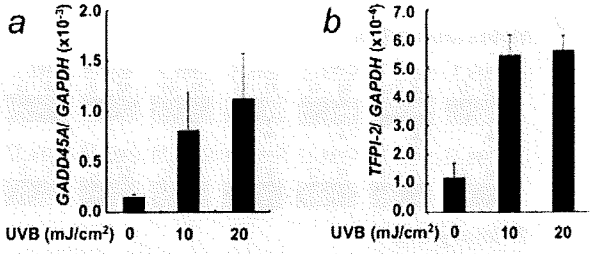

FIGURE 2 – *TFPI-2* expression after irradiation of HEMs to UVB. (*a*) *GADD45A* induction in response to UVB irradiation was first confirmed. Bars, SD. (*b*) *TFPI-2* expression was found to be induced by UVB 10 and 20 mJ/cm^2 irradiation. Bars, SD.

TABLE II – METHYLATION STATUS AND IMMUNOREACTIVITY OF TFPI-2 IN SURGICAL SPECIMENS

Specimen number	Origin	Methylation status	Immunoreactivity
1	Skin metastasis	M	–
2	Skin metastasis	M/U	–
3	Skin metastasis	M	–
4	Lung metastasis	M	–
5	Lymph node metastasis	M/U	–
6	Skin metastasis	U	NA
7	Skin metastasis	U	NA
8	Lung metastasis	U	+
9	Lymph node metastasis	U	+
10	Lymph node metastasis	U	+
11	Lymph node metastasis	U	+
12	Lymph node metastasis	U	–
13	Lymph node metastasis	U	–
14	Lymph node metastasis	U	–
15	Lymph node metastasis	U	–
16	Lymph node metastasis	U	NA
17	Lymph node metastasis	U	NA
18	Primary	U	+
19	Primary	U	+
20	Primary	U	+
21	Primary	U	+
22	Primary	U	+
23	Primary	U	+
24	Primary	U	+
25	Primary	U	–
26	Primary	U	–
27	Primary	U	–
28	Primary	U	–
29	Primary	U	–
30	Primary	U	–
31	Primary	U	NA
32	Primary	U	NA
33	Primary	U	NA
34	Primary	U	NA
35	Primary	U	NA
36	Primary	U	NA
37	Primary	U	NA

–, negative immunoreactivity for TFPI-2; +, positive immunoreactivity for TFPI-2; NA, not analyzed. Methylation of the *TFPI-2* promoter CGI was observed specifically in metastatic site specimens, not in primary site specimens ($p = 0.009$). No significant differences were seen in immunoreactivity between primary and metastatic specimens ($p > 0.05$, χ^2 test).

body (biotinylated anti-mouse IgG antibody) at a dilution of 250-fold at room temperature for 40 min. Melanin color was removed by placing the slides in 0.5% sodium azide at 4°C for 3–5 days. The binding of the second antibody was visualized by a Vectastain Elite ABC kit (Vector Laboratories, Burlingame, CA). Slides were counterstained with hematoxylin. As a negative control, absence of staining without the primary antibody was confirmed. As a positive control, staining of vascular epithelium was confirmed.[22]

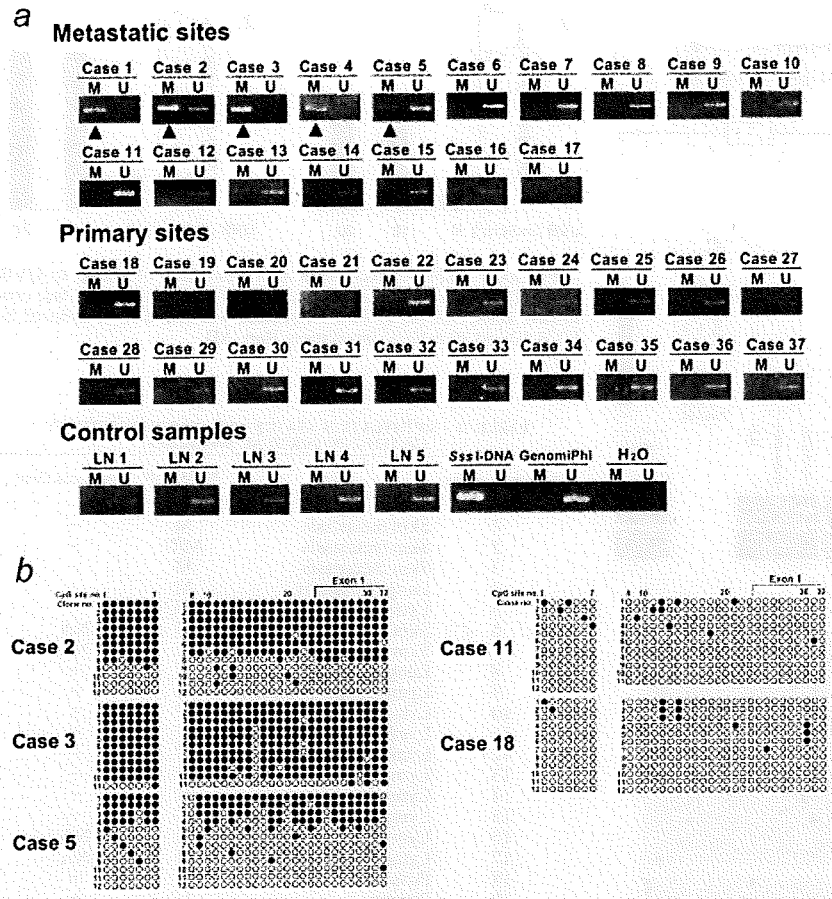

FIGURE 3 – Methylation statuses of the *TFPI-2* promoter CGI in surgical melanoma specimens. (*a*) MSP of the *TFPI-2* promoter CGI in 37 surgical melanoma specimens and 5 normal lymph nodes (LN). *Sss*I-DNA: fully methylated DNA; GenomiPhi: fully unmethylated DNA; M: primers specific to methylated DNA; and U: primers specific to unmethylated DNA. Arrowheads show bands obtained with primers specific to methylated DNA. (*b*) Bisulfite sequencing of the *TFPI-2* promoter CGI in representative surgical melanoma specimens. Cases 2, 3 and 5 had methylation by MSP, and cases 11 and 18 did not. Thirty-two CpG sites were analyzed in 2 separate PCR due to sample degradation. For each sample, 10 or more clones were sequenced. Closed and open circles show methylated and unmethylated CpG sites, respectively.

Statistical analysis

The differences in the incidences between the primary sites and metastatic sites were compared by a χ^2 test.

Results

Chemical genomic screening and identification of 18 genes with promoter methylation

Oligonucleotide microarray analyses were performed using RNA obtained from human melanoma cells with and without 5-aza-dC treatment. HMV-I, MeWo and WM-115 cell lines had 107, 112 and 16 genes, respectively, that (*i*) had signal intensities of 50 or less in nontreated cells and 100 or more in treated cells, and (*ii*) showed an increase of 16-fold or more. Genomic structures and chromosomal localizations were analyzed for these genes and 38, 35 and 6 genes (total 79 genes), respectively, were found to have CGIs in their 5′ regions, and not located on chromosome X, which harbors many normally methylated genes.[23]

Methylation statuses of the putative promoter CGIs of these 79 genes were analyzed by MSP in HEM and 8 melanoma cell lines, including HMV-I, MeWo and WM-115. Eighteen of them were found to be completely methylated (without unmethylated DNA molecules) in 1 or more of the 8 melanoma cell lines, but not in HEM (Table I).

Methylation and expression analysis of the 18 genes, and identification of TFPI-2

mRNA expression of the 18 genes was analyzed in 12 melanoma cell lines and HEM by quantitative RT-PCR, and association between methylation and transcriptional repression was examined. It was found that 9 genes were not expressed in HEM, that 7 genes (*APM2, FKBP1B, GSTM4, ISYNA1, PDLIM4, TFPI-2* and *TPM2*) were expressed in HEM and consistently repressed in melanoma cell lines with complete methylation, and that 2 genes (*ADFP* and *MT1K*) were expressed even in melanoma cell lines with complete methylation.

Among the 7 genes that had consistent association between methylation and transcriptional repression, *TFPI-2* was known to possess growth-suppressive functions[24–28] and to be silenced in gliomas, choriocarcinomas, pancreatic cancers and lung cancers.[28–31] Therefore we decided to focus on *TFPI-2* as a candidate tumor-suppressor gene silenced in malignant melanomas.

TFPI-2 minimal promoter activity was reported between −224 and −139 from the transcription initiation site[32] (Fig. 1*a*), and the methylation status of the region was confirmed by new sets of MSP primers (Fig. 1*b*). The same results with the initial screening were obtained. *TFPI-2* was completely methylated in HMV-I, partially methylated (both methylated and unmethylated DNA detected) in GAK, VMRC-MELG and C32TG, and completely unmethylated in the other 8 melanoma cell lines and HEM. *TFPI-2* was not expressed in HMV-I, but was expressed in most melanoma cell lines with unmethylated DNA molecules. Reexpression of *TFPI-2* by treatment of HMV-I with 5-aza-dC was confirmed by quantitative RT-PCR analysis (Fig. 1*c*). Further, the results by MSP were confirmed by bisulfite sequencing (Fig. 1*d*). The promoter region of *TFPI-2* was densely methylated in all DNA molecules in HMV-I, while it was unmethylated in 2 melanoma cell lines (MeWo and A2058) with high *TFPI-2* expression and HEM.

These results showed that *TFPI-2* was silenced by methylation of its promoter CGI in a melanoma cell line.

TFPI-2 *induction in response to UVB irradiation*

In a steady-state culture, HEM expressed *TFPI-2* mRNA only at a low level. It is generally difficult to distinguish genes that are functional in a tissue, even with low expression levels, such as *Rb*, *BRCA1* and *HIF-1*,[33–35] from genes that are not functional in a tissue and have little expression.[36] To make the distinction, it was considered informative to examine whether or not *TFPI-2* expression can be induced in response to cellular stress. Therefore, HEMs were irradiated with increasing doses of UVB. The effect of UVB irradiation was confirmed by observing induction of *GADD45A* mRNA expression (Fig. 2*a*). It was found that *TFPI-2* expression was induced at 4.2-fold after treatment with 10 mJ/cm^2 and 4.6-fold after that with 20 mJ/cm^2 in 3 independent treatments (Fig. 2*b*).

TFPI-2 *methylation and loss of expression*

Methylation of the *TFPI-2* promoter CGI was analyzed in 37 surgical melanoma specimens (17 metastatic site and 20 primary site specimens) and 5 normal lymph nodes (negative controls) by MSP. Methylation was detected only in 5 of the 17 metastatic site specimens (29%), while none in the primary site specimens ($p = 0.009$, χ^2 test) (Table II and Fig. 3*a*). Further, the result was confirmed by bisulfite sequencing in 5 representative specimens (Fig. 3*b*).

Immunohistochemical analysis of TFPI-2 was then performed on 26 surgical melanoma specimens, including the 5 specimens with methylated DNA and 21 specimens without methylated DNA. The remaining 11 of the 37 specimens were excluded due to excessive melanin deposition even after demelanization or unavailability of tissue sections. Five of the 5 specimens with methylated DNA and 10 of the 21 specimens without lacked immunoreactivity for TFPI-2 (representative results in Fig. 4). The remaining 11 specimens had TFPI-2 immunoreactivity (52%).

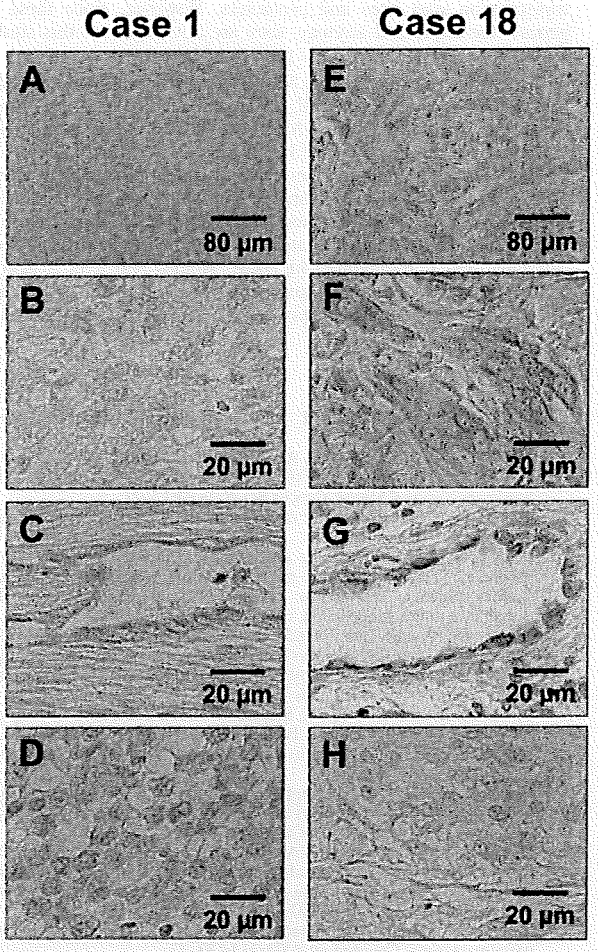

FIGURE 4 – Representative results of TFPI-2 immunohistochemical analysis in surgical melanoma specimens. Case 1 with methylated DNA showed no immunoreactivity (*a*,*b*) while case 18 without methylated DNA showed it (*e*,*f*). Staining of the vascular endothelium on the same slices was confirmed as positive controls (*c*,*g*). Absence of immunoreactivity was confirmed without anti-TFPI-2 antibody as negative controls (*d*,*h*).

Discussion

TFPI-2 silencing in human malignant melanomas was identified by a genome-wide screening using demethylation by 5-aza-dC and oligonucleotide microarray analysis. Transcriptional silencing of *TFPI-2* by promoter methylation has been recently reported in glioma,[29] choriocarcinoma,[30] pancreatic ductal adenocarcinoma[28] and nonsmall cell lung cancer.[31] In malignant melanoma, silencing by promoter methylation has not been reported, but TFPI-2 is known to suppress the invasiveness of amelanotic melanomas.[24] Our finding that methylation of the *TFPI-2* promoter CGI was present in 5 of 37 surgical melanoma specimens (13.5%) showed that silencing by promoter methylation is one of the mechanisms for *TFPI-2* inactivation in malignant melanomas.

TFPI-2, also known as placental protein (PP5) and matrix-associated serine protease inhibitor (MSPI), is a 32 kDa Kunitz-type serine proteinase inhibitor and an extracellular matrix protein that inhibits plasmin.[37] Since plasmin is involved in activation of matrix metalloproteinases (MMPs),[38] TFPI-2 can inhibit MMPs, which are known to be involved in tumor progression.[39] In various malignancies, such as choriocarcinoma, glioma, prostate cancer and lung cancer, tumor-suppressive functions of TFPI-2 have been demonstrated.[25,26,40,41] Additionally, Konduri *et al.* demonstrated that cell invasion and migration in melanomas can also be repressed by *TFPI-2* introduction.[24] In the present study, methylation of the *TFPI-2* promoter CGI was observed exclusively in metastatic site specimens ($p = 0.009$), and it was suggested that silencing of *TFPI-2* is one of the mechanisms for melanoma metastasis.

Distinction between a tumor-suppressor gene and a gene that has been methylated as a secondary event of tumorigenesis is important when a gene that appears to be silenced by promoter methylation is identified.[15] Tumor-suppressor genes tend to have low expression levels in the normal steady-state, but are often induced in response to cellular stresses.[33–35] At the same time, genes with little transcription in a tissue, most of which are not functional in the tissue, tend to be methylated in tumor cells.[36] For the distinction, in the present study, induction of *TFPI-2* expression in response to UVB irradiation, possibly through MAP kinase signaling activation,[42] was examined in HEMs.[43] *TFPI-2* expression was found to be induced by UVB, which is one of the most common causes of malignant melanomas and also induces apoptosis.[44] This suggested that *TFPI-2* could have a tumor-suppressive function and exert it through its roles in responding to cellular stresses, including induction of apoptosis.[27]

In the screening process of silenced genes, 2 genes (*ADFP* and *MT1K*) were found to be expressed even in melanoma cell lines with complete methylation. This was considered to be due to temporarily assigned transcription start sites in the database, or due to the presence of unidentified alternative promoters. Such inconsistency is usually solved by experimental identification of the exact

transcription start sites and promoters. However, since these 2 genes were expressed anyway, they are not targets of this study and such experiments were not performed here.

In our previous study, using MS-RDA with 3 methylation-sensitive restriction enzymes, *Hpa*II, *Sac*II and *Nar*I, putative promoter CGIs of 5 genes derived from MeWo were found to be completely methylated in at least 1 of 13 melanoma cell lines, but not in HEM.[13] However, among the 5 genes, none was expressed in HEM. On the other hand, in the present study, using a chemical genomic screening, we identified 5 genes whose putative promoter CGIs were completely methylated in 1 or more of the 8 melanoma cell lines, but unmethylated in HEM. Among the five, 2 genes (*AMP2* and *TPM2*) were expressed in HEM and were considered to be candidate tumor-suppressor genes. There was no overlap between the 5 genes identified by MS-RDA and the 5 genes identified by chemical genomic screening. These results suggested that different genes are identified by the 2 different approaches.

In conclusion, it was demonstrated for the first time in this study that *TFPI-2* is silenced by methylation of its promoter CGI in malignant melanomas. The specific presence of its methylation in metastatic sites suggested that its silencing is one of the mechanisms for melanoma metastasis.

Acknowledgements

Y.N. is a recipient of a Research Resident Fellowships from the Foundation for Promotion of Cancer Research.

References

1. Tucker MA, Goldstein AM. Melanoma etiology: where are we? Oncogene 2003;22:3042–52.
2. Tsuruo T, Naito M, Tomida A, Fujita N, Mashima T, Sakamoto H, Haga N. Molecular targeting therapy of cancer: drug resistance, apoptosis and survival signal. Cancer Sci 2003;94:15–21.
3. Flaherty KT. New molecular targets in melanoma. Curr Opin Oncol 2004;16:150–4.
4. Omholt K, Karsberg S, Platz A, Kanter L, Ringborg U, Hansson J. Screening of N-*ras* codon 61 mutations in paired primary and metastatic cutaneous melanomas: mutations occur early and persist throughout tumor progression. Clin Cancer Res 2002;8:3468–74.
5. Albino AP, Nanus DM, Mentle IR, Cordon-Cardo C, McNutt NS, Bressler J, Andreeff M. Analysis of ras oncogenes in malignant melanoma and precursor lesions: correlation of point mutations with differentiation phenotype. Oncogene 1989;4:1363–74.
6. Davies H, Bignell GR, Cox C, Stephens P, Edkins S, Clegg S, Teague J, Woffendin H, Garnett MJ, Bottomley W, Davis N, Dicks E, et al. Mutations of the *BRAF* gene in human cancer. Nature 2002;417:949–54.
7. Grafstrom E, Egyhazi S, Ringborg U, Hansson J, Platz A. Biallelic deletions in *INK4* in cutaneous melanoma are common and associated with decreased survival. Clin Cancer Res 2005;11:2991–7.
8. Maelandsmo GM, Florenes VA, Hovig E, Oyjord T, Engebraaten O, Holm R, Borresen AL, Fodstad O. Involvement of the pRb/p16/cdk4/cyclin D1 pathway in the tumorigenesis of sporadic malignant melanomas. Br J Cancer 1996;73:909–16.
9. Rodolfo M, Daniotti M, Vallacchi V. Genetic progression of metastatic melanoma. Cancer Lett 2004;214:133–47.
10. van der Velden PA, Metzelaar-Blok JA, Bergman W, Monique H, Hurks H, Frants RR, Gruis NA, Jager MJ. Promoter hypermethylation: a common cause of reduced *p16(INK4a)* expression in uveal melanoma. Cancer Res 2001;61:5303–6.
11. Spugnardi M, Tommasi S, Dammann R, Pfeifer GP, Hoon DS. Epigenetic inactivation of *RAS association domain family protein 1 (RASSF1A)* in malignant cutaneous melanoma. Cancer Res 2003;63:1639–43.
12. van der Velden PA, Zuidervaart W, Hurks MH, Pavey S, Ksander BR, Krijgsman E, Frants RR, Tensen CP, Willemze R, Jager MJ, Gruis NA. Expression profiling reveals that methylation of TIMP3 is involved in uveal melanoma development. Int J Cancer 2003;106:472–9.
13. Furuta J, Nobeyama Y, Umebayashi Y, Otsuka F, Kikuchi K, Ushijima T. Silencing of *peroxiredoxin 2* and aberrant methylation of 33 CpG islands in putative promoter regions in human malignant melanomas. Cancer Res 2006;66:6080–6.
14. Gallagher WM, Bergin OE, Rafferty M, Kelly ZD, Nolan IM, Fox EJ, Culhane AC, McArdle L, Fraga MF, Hughes L, Currid CA, O'Mahony F, et al. Multiple markers for melanoma progression regulated by DNA methylation: insights from transcriptomic studies. Carcinogenesis 2005;26:1856–67.
15. Ushijima T. Detection and interpretation of altered methylation patterns in cancer cells. Nat Rev Cancer 2005;5:223–31.
16. Choi MH, Lee IK, Kim GW, Kim BU, Han YH, Yu DY, Park HS, Kim KY, Lee JS, Choi C, Bae YS, Lee BI, et al. Regulation of PDGF signalling and vascular remodelling by peroxiredoxin II. Nature 2005;435:347–53.
17. Suzuki H, Gabrielson E, Chen W, Anbazhagan R, van Engeland M, Weijenberg MP, Herman JG, Baylin SB. A genomic screen for genes upregulated by demethylation and histone deacetylase inhibition in human colorectal cancer. Nat Genet 2002;31:141–9.
18. Yamashita S, Tsujino Y, Moriguchi K, Tatematsu M, Ushijima T. Chemical genomic screening for methylation-silenced genes in gastric cancer cell lines using 5-aza-2′-deoxycytidine treatment and oligonucleotide microarray. Cancer Sci 2006;97:64–71.
19. Furuta J, Umebayashi Y, Miyamoto K, Kikuchi K, Otsuka F, Sugimura T, Ushijima T. Promoter methylation profiling of 30 genes in human malignant melanoma. Cancer Sci 2004;95:962–8.
20. Niwa T, Yamashita S, Tsukamoto T, Kuramoto T, Nomoto T, Wakazono K, Fujita H, Matsushima T, Tatematsu M, Sugimura T, Ushijima T. Whole-genome analyses of loss of heterozygosity and methylation analysis of four tumor-suppressor genes in *N*-methyl-*N*′-nitro-*N*-nitrosoguanidine-induced rat stomach carcinomas. Cancer Sci 2005;96:409–13.
21. Ogawa M, Yanoma S, Nagashima Y, Okamoto N, Ishikawa H, Haruki A, Miyagi E, Takahashi T, Hirahara F, Miyagi Y. Paradoxical discrepancy between the serum level and the placental intensity of PP5/TFPI-2 in *Preeclampsia* and/or intrauterine growth restriction: possible interaction and correlation with glypican-3 hold the key. Placenta 2006;28:224–32.
22. Iino M, Foster DC, Kisiel W. Quantification and characterization of human endothelial cell-derived tissue factor pathway inhibitor-2. Arterioscler Thromb Vasc Biol 1998;18:40–6.
23. Simpson AJ, Caballero OL, Jungbluth A, Chen YT, Old LJ. Cancer/testis antigens, gametogenesis and cancer. Nat Rev Cancer 2005;5:615–25.
24. Konduri SD, Tasiou A, Chandrasekar N, Nicolson GL, Rao JS. Role of tissue factor pathway inhibitor-2 (TFPI-2) in amelanotic melanoma (C-32) invasion. Clin Exp Metastasis 2000;18:303–8.
25. Konduri SD, Rao CN, Chandrasekar N, Tasiou A, Mohanam S, Kin Y, Lakka SS, Dinh D, Olivero WC, Gujrati M, Foster DC, Kisiel W, et al. A novel function of tissue factor pathway inhibitor-2 (TFPI-2) in human glioma invasion. Oncogene 2001;20:6938–45.
26. Konduri SD, Tasiou A, Chandrasekar N, Rao JS. Overexpression of tissue factor pathway inhibitor-2 (TFPI-2), decreases the invasiveness of prostate cancer cells *in vitro*. Int J Oncol 2001;18:127–31.
27. Tasiou A, Konduri SD, Yanamandra N, Dinh DH, Olivero WC, Gujrati M, Obeyesekere M, Rao JS. A novel role of tissue factor pathway inhibitor-2 in apoptosis of malignant human gliomas. Int J Oncol 2001;19:591–7.
28. Sato N, Parker AR, Fukushima N, Miyagi Y, Iacobuzio-Donahue CA, Eshleman JR, Goggins M. Epigenetic inactivation of TFPI-2 as a common mechanism associated with growth and invasion of pancreatic ductal adenocarcinoma. Oncogene 2005;24:850–8.
29. Konduri SD, Srivenugopal KS, Yanamandra N, Dinh DH, Olivero WC, Gujrati M, Foster DC, Kisiel W, Ali-Osman F, Kondraganti S, Lakka SS, Rao JS. Promoter methylation and silencing of the tissue factor pathway inhibitor-2 (TFPI-2), a gene encoding an inhibitor of matrix metalloproteinases in human glioma cells. Oncogene 2003;22:4509–16.
30. Hube F, Reverdiau P, Iochmann S, Rollin J, Cherpi-Antar C, Gruel Y. Transcriptional silencing of the TFPI-2 gene by promoter hypermethylation in choriocarcinoma cells. Biol Chem 2003;384:1029–34.
31. Steiner FA, Hong JA, Fischette MR, Beer DG, Guo ZS, Chen GA, Weiser TS, Kassis ES, Nguyen DM, Lee S, Trepel JB, Schrump DS. Sequential 5-Aza-2′-deoxycytidine/depsipeptide FK228 treatment induces tissue factor pathway inhibitor 2 (TFPI-2) expression in cancer cells. Oncogene 2005;24:2386–97.
32. Kamei S, Kazama Y, Kuijper JL, Foster DC, Kisiel W. Genomic structure and promoter activity of the human tissue factor pathway inhibitor-2 gene. Biochim Biophys Acta 2001;1517:430–5.
33. Spike BT, Macleod KF. The Rb tumor suppressor in stress responses and hematopoietic homeostasis. Cell Cycle 2005;4:42–5.
34. Gilmore PM, Quinn JE, Mullan PB, Andrews HN, McCabe N, Carty M, Kennedy RD, Harkin DP. Role played by BRCA1 in regulating